INTERIM REPORT BY THE WORKING GROUP ON EFFECTS

IMPACTS OF AIR POLLUTION ON ECOSYSTEMS, HUMAN HEALTH AND MATERIALS UNDER DIFFERENT GOTHENBURG PROTOCOL SCENARIOS

http://live.unece.org/env/lrtap/workinggroups/wge/30meeting_rev.htm

Cover photos (by AC Le Gall):

Arc de triomphe du Carrousel, Paris
Limed river in Norway
Wheat
Spring in Halatte Forest, France

EXECUTIVE SUMMARY

The objectives of this analysis, decided by the Bureau of the Working Group on Effects, are to:

1- Provide information on the effects of air pollution on ecosystems, human health and materials to support decisions for the revision of the Gothenburg protocol.

2- Demonstrate the application of new science and indicators, developed since 1999, to illustrate the potential impact of policy /decisions on the environment, human health and materials.

3- Illustrate the effectiveness of emission scenarios to improve the environment and human health

This analysis has been carried out by the International Cooperative Programmes (ICPs) and Task Force on Health under the Working Group on Effects (WGE) between October 2010 and February 2011. The analysis is based on scenarios of air pollutant emissions (S, N, O_3 and PM) provided by the Task Force on Integrated Assessment Modelling (TFIAM) and the European Monitoring and Evaluation Programme (EMEP) in October 2010 (described in CIAM report 1/2010). Relevant data was formatted by the Coordination Centre for Effects (CCE) in order to facilitate the ICPs modelling work and comparison with field data. Results have been presented and discussed at different meetings under the Long-range Transboundary Air Pollution Convention (LRTAP) between February and May 2011.

The scenarios referred to in this report are:

- NAT2000: historical data for the year 2000 based mainly on national information.
- NAT2020: data generated under a current legislation scenario for 2020 based mainly on national information about future economic projections.
- PRI2020 and PRI2030: data generated under a current legislation scenario for 2020 and 2030 and based mainly on economic projections developed by the PRIMES model.
- MTFR2020: data based on a scenario assuming all technically feasible technologies being implemented by 2020.

NAT and PRI projections are considered to represent “baseline” scenarios: they provide the emissions as they will happen if no new regulations are implemented. MTFR represents the reduction that would be obtained if the most stringent regulations were implemented. Any decision leading to some emission reduction will lead to a situation between the baseline and the MTFR scenario. Further details on these projections and scenarios are specified in CIAM report 1/2010.

Emissions scenarios have undergone some revisions since October 2010, mainly to respond to requests from the Working Group on Strategy and Review (WGSR). It is therefore expected that an update of this work will be carried out in the summer/autumn 2011 to ensure a close correlation to the emission scenarios that will be used in the latest stage of the Gothenburg protocol revision (expected at the end of 2011 or early 2012).

- ***Impacts and trends***

Air pollution regulations, including protocols of the LRTAP Convention, have led to significant decreases in sulphur and nitrogen concentrations in the air and in their deposition to ecosystems. The trends show that the sulphur emissions in Europe have decreased by more than 70 % in 2010 compared to 1980 while total nitrogen emissions have decreased by about 50 % in the same period (Figure 1). The consequences of these decreased emissions have been observed through the monitoring network designed under the LRTAP Convention and this report illustrates some of the results.

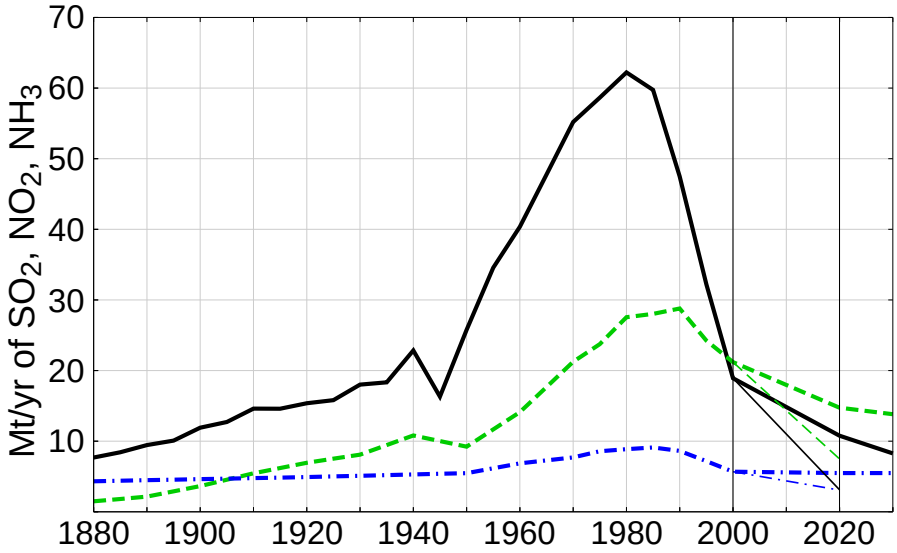

Figure 1:1880–2030 development of European emissions of S (solid line), oxidized N (dashed line) and reduced N (dashed-dotted line). From the year 2000 emissions are calculated with the NAT2000 scenario. Beyond 2020, the NAT2020 and PRI2030 scenarios are used. The thin lines point to the MTFR scenario for 2020. [Note: PRI2020 is very close to NAT2020]

The Working Group on Effects has, over several decades, developed, compiled and collated a large amount of multidisciplinary scientific knowledge related to the impact of air pollution on ecosystems, human health and materials The monitoring and modelling carried out by the ICPs and Task Forces enable analysis of the dynamics and trends of the biotic and abiotic parameters of ecosystems. Selected examples illustrate the impacts of the increase and decrease of air pollution on the environment. More results are available on the WGE and ICPs/TF web sites as well as in the scientific literature.

- ***Discussion and conclusion:***

The monitoring and the modelling carried out under the Working Group on Effects shows that the magnitude of the impact of air pollution will decrease under baseline (NAT2020 and PRI2020) and MTFR scenarios. However, as illustrated above and summarized below, none of the impacts considered (acidification, eutrophication, effects of ozone, material soiling and corrosion, human health effects) are expected to disappear by 2020 under either scenario.

Acidification

ICP Modelling and Mapping results suggest that acidification will be of concern in 2 to 4 % of the EMEP area. This is consistent with ICP Waters and ICP Integrated Monitoring, whose observations and modelling show that the most acidified sites will not recover by 2020. Moreover, ICP Forests calculations suggest that most ICP Forests sites will be protected from acidification under the baseline scenario and all will be protected under the MTFR scenario. However, a tendency towards low base cation saturation in forests soils is expected. In the long term, this may have deleterious consequences on the soil nutritional status as well as on the base cations supply to fresh waters.

Eutrophication

Eutrophication remains, and will remain, a widespread problem. In terrestrial ecosystems, excesses of nitrogen inputs leads to accumulation of nitrogen in soils and eventually leaching to waters. This can promote changes in species diversity and susceptibility of vegetation to insects, fungal diseases or drought. Calculations from ICP Modelling and Mapping were supported by assessments from ICP Integrated Monitoring and ICP Forests: in 2020, under the baseline scenario, more than 60 % of EU27 and 35 % of EMEP areas will still be at risk of eutrophication. The amplitude of the exceedances will range between 2 and 5 kg/ha/yr at ICP Integrated Monitoring sites which are situated in background areas distant from local sources. Maximum exceedance values (around 10 kg/ha/yr) were calculated for the Netherlands by ICP Modelling and Mapping. Also, as shown in Figure 4, under baselines projections, the proportion of eutrophic (C:N between 10-17) and hypertrophic (C:N smaller than 10) sites is expected to continue to increase at ICP Forests monitoring plots beyond 2020. Observations at ICP Integrated Monitoring sites give evidence on correlations between critical loads exceedances calculated with the NAT2000 scenario and measured parameters characterising acidification and eutrophication. This confirms the robustness of the critical loads methodology.

The contribution of ammonia to ecosystem damage is expected to remain important across Europe under the baseline scenario. In 2020, concentrations over most of Europe will remain greater than the critical level for lichen and bryophytes (1 µg/m^3) according to the baseline scenario. In large areas, especially in cattle raising areas (Brittany in France, the Netherlands, Northern Italy), average annual concentrations will remain greater than the critical limit for higher plants (2-4 µg/m^3).

Ozone

Ozone affects human health, natural vegetation, forests, grasslands and crops. ICP Vegetation has shown that ozone pollution may partly suppress the global carbon sink via its adverse effects on plant growth. It can also make vegetation less able to withstand periods of drought. Areas at particular risk of ozone impact are southern Europe, but also include most of central and southern parts of northern Europe. Projected air pollution reductions may lead to lower ozone concentrations but, under the NAT 2020 baseline scenario, for example, wheat yield losses may still be greater than 5 % in more than 80 % of the EMEP grid squares. The Task Force on Health showed that currently in the EU25 there are 21,000 premature deaths every year due to high ozone concentrations (>35 ppb or 70 µg/m^3). Only a small decrease in this premature death number is expected with the full implementation of the current legislation.

Particulate matter

Particulate matter (PM) causes respiratory and cardiovascular mortality and morbidity and over 300,000 premature deaths are attributed to them every year in Europe. In the US, a recent study demonstrated that health improvement was associated with the decrease of PM levels over 20 years. In this study, a 7.3 months increase in life expectancy was attributed to a decrease of $PM_{2.5}$ by 10 $\mu g/m^3$. The Task Force on Health has compared the health risk associated with black carbon to that associated with $PM_{2.5}$. They concluded that although there is sufficient evidence of health risk associated with black carbon, it is insufficient to justify replacing $PM_{2.5}$ by black carbon as a health-relevant indicator of particulate air pollution.

Particulate matter and other air pollutants also cause soiling and corrosion, which damage building materials and cultural heritage sites. ICP Materials have established dose-response relationships and proposed targets for 2020 and 2050. These targets correspond to tolerable levels of corrosion or soiling. For instance, the proposed tolerable level for soiling results in PM10 levels less than 20 $\mu g/m^3$ for 2020 and less than 10 $\mu g/m^3$ for 2050. Calculations done at the scale of the EMEP grid (50x50 km²) suggest that with the baseline scenario, the more stringent 2050 targets would be achieved on nearly 88 % of the EMEP area, while on almost all of the remaining 12 % the 2020 targets would be achieved. Comparisons with field data, however, show that these calculations are too optimistic and that urban areas are pollution hotspots which are likely to remain at higher risk than shown at the 50x50 km² grid scale used in this assessment.

Economic impacts and impacts on ecosystem services

Currently economic impact assessments are performed in the GAINS model only for human health indicators. However, several of the ICPs are developing their work towards associating the impacts described above to ecosystem services or economic costs, or both. Recent data from ICP Vegetation suggests economic losses of more than three billion euros, due to ozone damage to Europe's most extensively grown crop, wheat. ICP Materials indicators may also be associated with specific costs in the future. Impacts on air pollution on ecosystems may be evaluated, in terms of availability of drinking water, resilience of forests to pest attack, to drought (which may have a cost in term of wood quality), to quality of recreational areas (with, for instance, the impact on recreational fisheries).

In summary, even after full (hypothetical) implementation of the MTFR scenario for 2020, many areas would remain at risk from the adverse impacts of air pollution on ecosystems (including crops), human health and materials. Thanks to air pollution regulations implemented since the 1980s, acidification will be of least concern in the future. However, considerable adverse impacts of eutrophication (nitrogen pollution), ozone and particulate matter (including black carbon) will remain over large areas of Europe.

CONTENTS

EXECUTIVE SUMMARY **3**

CONTENTS **7**

LIST OF TABLES **11**

GLOSSARY **12**

Acronyms 12

Definitions 13

1. INTRODUCTION AND AIMS **14**

2. SCENARIOS **15**

2.1 Short description of the different scenarios 15

2.2 Further scenarios developed by the TF IAM 15

3. ICPS AND TASK FORCE RESULTS **16**

3.1 ICP Forests 16

3.2 ICP Waters 21

3.3 ICP Integrated Monitoring 28

3.3.1 Assessments of critical loads at ICP IM sites 28

3.3.2 Comparison of exceedance of critical loads with empirical effects indicators 30

3.4 ICP Modelling and mapping 32

3.4.1 Accumulated Average Exceedances and Area at risk of acidification and eutrophication 32

3.4.2 Risks in significant change of biodiversity 35

3.4.3 The risk of delayed effects relative to 2050 36

3.5 ICP Vegetation 38

3.5.1 Background 38

3.5.2 Policy-relevant effect indicators 38

3.5.3 Mapping different effect indicators using the various projections 39

3.5.4 Temporal trends 43

3.5.5 Ozone impacts in a changing climate beyond 2050 43

3.6 ICP Materials 44

3.7 Task force on health 47

4. DISCUSSION AND CONCLUSIONS **48**

4.1 Scientific knowledge: State of the art 48

4.2 On-going scientific progresses 49
4.3 Policies successes monitored by the Working Group on Effects 50
4.4 Scenarios analysis informs on the impact of future regulations 50

5. BIBLIOGRAPHY 52

LIST OF FIGURES

Figure 1:1880–2030 development of European emissions of S (solid line), oxidized N (dashed line) and reduced N (dashed-dotted line). From the year 2000 emissions are calculated with the NAT2000 scenario. Beyond 2020, the NAT2020 and PRI2030 scenarios are used. The thin lines point to the MTFR scenario for 2020. [Note: PRI2020 is very close to NAT2020]..... 4

Figure 2:1880–2030 development of European emissions of S (solid line), oxidized N (dashed line) and reduced N (dashed-dotted line). From the year 2000 emissions are calculated with the NAT2000 scenario. Beyond2020, the NAT2020 and PRIMES 2030 scenarios are used. Earlier data are from Schöpp et al. (2003). The thin lines point to the MFR scenario for 2020. [Note: PRIMES2020 is very close to NAT2020]..... 14

Figure 3: Exceedances of critical loads for acidity in the years 1980(a), 2000(b), and 2020 national projection (c), modelled by PRIMES (d), MFR scenario (e), and exceedance of critical loads by the latest known ICP Forests throughfall measurements (f)..... 17

Figure 4: The exceedance of critical loads for nutrient nitrogen in the years 1980(a), 2000(b), 2020 national projection (c), modelled by PRIMES (d), MFR scenario (e) and the latest known ICP Forests throughfall measurements (f)..... 19

Figure 5: Overall trend for base saturation classes modeled by VSD+..... 20

Figure 6: Overall trend for pH value modelled by VSD+ and classified by buffering classes (Ulrich 1981).. 20

Figure 7: Overall trend for C:N ratio modelled by VSD+ and classified by nutrient levels...... 21

Figure 8: Long-term deposition, lake chemistry and lake biology monitoring data for Lake Saudlandsvatn, an ICP Waters site in southern Norway. Shown are non-marine S (S*) deposition, lake ANC and pH, catch-per-unit effort of fish, number of specimens collected of the acid-sensitive mayfly B. rhodani, and % specimens collected of the acid-sensitive zooplankton species D. Longispina (Data from Hesthagen et al. 2011)...... 22

Figure 9: Concentrations of sulphate (SO_4) and ANC in Lake Saudlandsvatn measured (red squares) and simulated (blue diamonds) with the MAGIC model. The future simulated values assume S* deposition as specified by the NAT scenario for 2000 and 2020, and constant level past the year 2020..... 23

Figure 10: Non-marine S and N (oxidised and reduced) deposition scenarios used to drive the MAGIC model and the resulting ANC projections at the Lake Saudlandsvatn, southern Norway. Also shown are the annual observed ANC concentrations (red squares) and the ANC_{limit} for brown trout in the lake (dashed line)...... 25

Figure 11: Map of Europe showing the location of the 9 ICP Waters sites used with the MAGIC model for the present assessment...... 26

Figure 12: ANC concentrations at ICP Waters sites in Europe as simulated by MAGIC under several scenarios of future S and N deposition (lines). Observed depositions are shown (red squares). See Table 1 for site details...... 27

Figure 13: Number of plots in ICP IM sites that are protected/not protected for eutrophication (according to calculations based on empirical critical loads) assuming different deposition scenarios...... 29

Figure 14: Exceedance of critical load for acidification ($ExCL_A$, eq ha^{-1} yr^{-1}, NAT2000 scenario, x-axis) for aquatic ecosystems vs. annual median fluxes (left column) and concentrations (right column) measured between 2002 and 2006 (y-axis) of ANC, H^+ and non-marine sulphate (xSO_4) in runoff for 14 ICP IM sites. Negative exceedance values are included in graphs in order to show the difference between deposition and critical load value, also in the case that CL is greater than deposition...... 31

Figure 15: Exceedance of critical load for mass balance nutrient nitrogen ($ExCL_{nut}N$, eq ha^{-1} yr^{-1}) (x-axis) vs. median annual fluxes (left down) and concentration (left upper) (2002-2006) (y-axis) of NO3 in runoff for 13-20 ICP IM sites, and exceedance of empirical values of critical load for nutrient nitrogen ($ExCL_{emp}N$, eq ha^{-1} yr^{-1}) (x-axis) vs. median annual fluxes (right down) and concentrations (right up) (2002-2006) (y-axis) of NO3 in runoff for 16-23 ICP IM sites. Exceedance values were calculated using the NAT2000 deposition scenario. Negative exceedance values are included in graphs in order to show the difference between deposition and critical load value, also in the case that CL is greater than deposition. 32

Figure 16: Average Accumulated Exceedance (AAE) of critical loads for acidification in 2000 (left) and 2020 under the Baseline Scenario (middle) and Maximum feasible reductions (right). Peaks of exceedances in 2000 on the Dutch-German border and in Poland (red shading) are reduced in 2020, as is the area at risk in general (size of shaded area in grid cells). 34

Figure 17: Average Accumulated Exceedance (AAE) of critical loads for eutrophication in 2000 (left), and in 2020 (NAT2020 data, middle) and MFR (MFR2020 data, right). The areas with peaks of exceedances in 2000 (red shading) are markedly decreased in 2020. However, area at risk of nutrient nitrogen (size of shades indicates relative area coverage) remain widely distributed over Europe in 2020, even under MFR. 34

Figure 18: Ammonia concentrations under four projections and scenarios between 2000 and 2030. Critical limits for lichens and bryophytes is set at 1µg.m^{-3}. Critical limits for higher plants are set between 2 and 4 µg.m^{-3} (UBA, 2004, updated). 35

Figure 19: Change in biodiversity (all ecosystems) greater than 5%, caused by nitrogen deposition and evaluated with the NAT2000, NAT 2020 and MFR 2020 data sets. 36

Figure 20: Four combinations of critical load (non-)exceedance and criterion (non-)violation. RDT: recovery delay time. DDT: damage delay time. 37

Figure 21: The risk of adverse ozone impacts in 2000 a) on biomass production in forest concentration-based AOT40 for forest trees (the AOT40-based critical level is 5 ppm.h), b) on human health as indicated by SOMO35, c) on generic deciduous tree as calculated by the flux model (POD1). The maps were produced using the NAT 2000 projection and colour classes have been scaled in the same way for each metric based on the highest values to allow direct comparison.....40

Figure 22: The risk of adverse ozone impacts on biomass production in forest using the generic deciduous tree flux model (POD_1) for a) NAT2000, b) NAT2020, c) MFR2020. Colour classes have been scaled in the same way for each metric based on the highest values to allow direct comparison.....40

Figure 23: Proportion of grid squares within specified categories of POD1 calculated using the generic forest flux model as calculated with the different datasets.....41

Figure 24:: Predicted economic losses for ozone effects on wheat in million € per 50 x 50 km² grid square in (a) 2000 and (b) 2020 for the wheat growing areas of EU27+CH+NO as indicated by the NAT scenario and flux-based methodology (from Mills and Harmens, 2011). 42

Figure 25: Predicted economic losses for effects on tomato in million Euro per 50 x 50 km grid square in (a) 2000 and (b) 2020 for the tomato growing areas of EU27+CH+NO (> 1 t yield per square) as indicated by the NAT scenario and flux-based methodology(from Mills and Harmens, 2011). 42

Figure 27: Compliances of targets of indicators for materials calculated from dose – response relationships for 2020 (light grey: All 2050 targets met; dark grey: All 2020 targets met (but 2050 targets not met); black: No target met for at least one indicator). 46

LIST OF TABLES

Table 1: Locations of ICP Waters sites used for the assessment of the different projections. 26

Table 2: Summary of biological status in the study lakes observed (1990, 2000, 2010) and forecast recovery under the old CLE and ex-post scenarios. Recovery classes: 0 no recovery; * start recovery; ** partial recovery; * full recovery. Organism groups: f = fish; zp = zooplankton; zb = zoobenthos; dia = diatoms. NS: not significant..... 28**

Table 3: Average exceedance of critical loads of acidification CL_A (eq/ha/yr) and eutrophication CLnutN and CLempN (eq/ha/yr and kg/ha/yr). 1995: Deposition modelled by EMEP. Future deposition estimates according to the NAT2000, NAT2020, PRI2020, PRI2030 and MFR2020 datasets. 29

Table 4: Evolution of the areas at risk of acidification and eutrophication in Europe according to the scenarios baseline (NAT) and MFR. All % refer to the whole EU27 or European areas. 33

Table 5: Evolution of the Accumulated Average Exceedance of critical loads for acidification and eutrophication (eq ha^{-1} yr^{-1}) in Europe according to the baseline (NAT) and MFR scenarios. 34

Table 6: Areas tentatively computed to be at risk of a significant* change of biodiversity in 2000 (col. II), in 2020 under the Baseline (col. III) and in 2020 under the Maximum Feasible Reductions (MFR) scenario (col. IV). The area at risk of a significant change of biodiversity in Europe in 2000, Baseline 2020 and MFR 2020 is about 5%, 2% and 0% respectively (last row). The improvement of the protection against the significant change of biodiversity under NAT2020 and MFR compared to 2000 is 4% (col. V) and 5% (col. VI) respectively. 36

Table 7: Natural areas in Europe with an RDT and DDT before or after 2050, under both NAT2020 and MFR2020, expressed as percentage of the area where critical loads for eutrophication are exceeded under baseline scenario in 2020. 37

Table 8: Predicted impacts of ozone pollution on wheat and tomato yield and economic value, together with critical level exceedance in EU27+Switzerland+Norway in 2000 and 2020 under the current legislation scenario (NAT scenario). Analysis was conducted on a 50 x 50 km EMEP grid square using crop values in 2000 and an ozone stomatal flux-based risk assessment (From Mills and Harmens, 2011). 43

Table 9: Targets for protecting materials of infrastructure and cultural heritage for 2020 and 2050 (ECE/EB.AIR/WG.1/2009/16 "Indicators and targets for air pollution effects") 44

Table 10: Compliances of targets of indicators for materials calculated from dose-response relationships for the whole EMEP region in 2020. 45

Table 11: Comparison of field observations of SO_2 and corrosion of carbon steel, zinc and limestone at ICP Materials test sites for the year 2000 ("Field") and values for the same parameters calculated from the NAT 2000 dataset ("Nat") for the corresponding grid cells. 46

GLOSSARY

ACRONYMS

AAE	Average Accumulated Exceedance of a critical load.
ACS	American Cancer Society
ANC	Acid neutralising capacity. Defined as equivalent sum of base cations (Ca, Mg, Na, K) minus equivalent sum of strong acid anions (SO_4, Cl, NO_3). Units: µeq/l. ANC is a measure of degree of acidification of water.
ANC_{limit}	the lowest ANC concentration that does not damage an indicator organism
CCE	Coordination Centre for Effects
CL_A	Critical load of acidity.
$CL_{emp}N$	Empirical critical loads of nutrient nitrogen
$CL_{nut}N$	Critical load of nutrient nitrogen
EMEP	Cooperative Programme for Monitoring and Evaluation of the Long-range Transmission of Air Pollutants in Europe
CIAM	Centre for integrated assessment modelling at the International Institute for Applied System Analysis (Austria)
CLE	Current LEgislation (scenario)
GAINS	Greenhouse gas – Air pollution Interactions and Synergies model
HIA (TFH)	health impact assessment
LRTAP	(Convention on) Long-range Transboundary Air Pollution
MAGIC	Model for Acidification of Groundwater In Catchments
MFR	Maximum feasible reduction
NAT	Emission scenario based on data provided by each party (national data)
POD_y	Phytotoxic ozone dose above a flux threshold of Y nmol m^{-2} s^{-1}
PRI	Emission scenario based on data calculated by the PRIMES model
PRIMES	Energy Systems Model of the National Technical University of Athens
S*	Non-marine sulphur (deposition)
TFIAM	Task Force on Integrated Assessment Modelling
WGE	Working Group on Effects under the Convention on Long-range Transboundary Air Pollution
WGSR	Working Group on strategies and review under the Convention on Long-range Transboundary Air Pollution

DEFINITIONS

AOT40: The sum of the differences between the hourly mean ozone concentration (in ppb) and 40 ppb when the concentration exceeds 40 ppb in daylight hours, accumulated over a stated time period. Units: ppb h or ppm h.

Critical load: a quantitative estimate of an exposure to one or more pollutants below which significant harmful effects on specified sensitive elements of the environment do not occur according to present knowledge.

Equivalents: Concentrations units representing the acidification or eutrophication potential of a compound.

	mol	equivalent	g of x (x= S, N or H)
SO_4^{2-}	1	2	32
NO_3^-	1	1	14
H^+	1	1	1

Hypertrophic: refers to ecosystems with high nutrients concentrations, generally leading to eutrophication.

Mesotrophic: refers to ecosystems with an intermediate level of productivity.

Oligotrophic: refers to ecosystems that are poor in nutrients.

Phytotoxic Ozone Dose (POD_Y): the phytotoxic ozone dose is the accumulated ozone flux into leaf pores (stomatal flux, F_{st}) above a flux threshold of Y nmol m^{-2} s^{-1}, accumulated over a stated time period during daylight hours. (Note this parameter was formerly named $AF_{st}Y$). Units: mmol m^{-2} PLA where PLA is the projected leaf area.

Stomatal flux of ozone (F_{st}): This term describes the uptake of ozone through pores in the leaf surface (stomata). It is calculated from the effects of climate (temperature, humidity, light), ozone, soil (moisture availability) and plant development (growth stage) on the extent of opening of the stomata. F_{st} is normally calculated from the hourly mean values and is regarded in this context as the hourly mean flux of ozone through the stomata. Units nmol m^{-2} PLA s^{-1}.

SOMO35: the sum of the maximum 8-hour ozone concentrations over 35 ppb (= 70 µg/m^3), a measure of accumulated annual ozone concentrations used as an indicator of health hazards. Units: ppm h

1. INTRODUCTION AND AIMS

Air pollution regulations, including protocols of the Convention on Long-range Transboundary Air Pollution (LRTAP), have lead to significant decreases in sulphur and nitrogen concentrations in the air and in their deposition on ecosystems. Sulphur emissions in Europe have decreased by about 70% between 1980 and 2010 while total nitrogen emissions decreased by about 50% (Figure 1).

The consequences of these decreased emissions have been observed through the monitoring network designed under the LRTAP Convention. Data showing significant downward trends in sulphur deposition have been collected in forests (Fischer et al, 2010) and in watersheds away from local sources (Hesthgen et al, 2011; Skjelkvåle and de Wit, 2008). Trends for nitrogen depositions are not as general and are less marked. As for ozone, although peak levels have declined in recent decades in Europe, background concentrations are rising due to hemispheric transport from other regions of the globe (Royal Society, 2008).

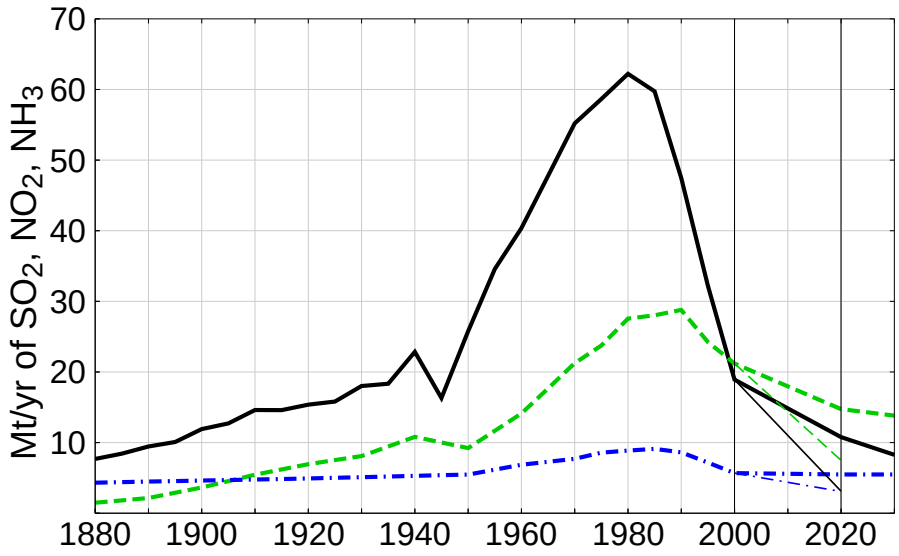

Figure 2:1880–2030 development of European emissions of S (solid line), oxidized N (dashed line) and reduced N (dashed-dotted line). From the year 2000 emissions are calculated with the NAT2000 scenario. Beyond2020, the NAT2020 and PRIMES 2030 scenarios are used. Earlier data are from Schöpp et al. (2003). The thin lines point to the MFR scenario for 2020. [Note: PRIMES2020 is very close to NAT2020]

The LRTAP Convention has adopted several protocols, including the multi-pollutant/multi-effects Gothenburg protocol in 1999 to abate acidification, eutrophication and ground-level ozone. Its revision has started in 2007. On-going discussions are based on scientific work made available to stakeholders.

The Working Group on Effects (WGE) set under the LRTAP Convention has continuously provided scientific information on the state of the environment to other bodies in the Convention, and in particular to the Working Group on Strategies and Review (WGSR) and to the Executive Body (EB). Since 1999 and the first Gothenburg protocol, tools, observations capacities, modelling performances have been developed and improved so that it is now possible to provide a comprehensive overview of the situation and to forecast changes to come.

This interim report describes the results obtained with new and updated indicators by the WGE for the emission projections supplied by the Centre of Integrated Assessment Modelling (CIAM) in October 2010. It should be seen as complementary to the information provided by GAINS and reported in CIAM's reports (Amann et al, 2010, Amann et al, 2011). This report will be finalised with updated scenarios data when they become available (2nd semester 2011).

2. SCENARIOS

2.1 SHORT DESCRIPTION OF THE DIFFERENT SCENARIOS

The scenarios referred to in this report are:

- NAT2000: historical data for the year 2000 based mainly on national information.
- NAT2020: data generated under a current legislation scenario for 2020 based mainly on national information about future economic projections.
- PRI2020 and PRI2030: data generated under a current legislation scenario for 2020 and 2030 and based mainly on economic projections developed by the PRIMES model.
- MTFR2020: data based on a scenario assuming all technically feasible technologies being implemented by 2020.

NAT and PRI projections are considered to represent "baseline" scenarios: they provide the emissions as they will happen if no new regulations are implemented. MTFR represents the reduction that would be obtained if the most stringent regulations were implemented. Any decision leading to some emission reduction will lead to a situation between the baseline and the MTFR scenario. Further details on these projections and scenarios are specified in CIAM report 1/2010.

ICPs have received five datasets with N, S, O_3 concentrations and depositions in October 2010 issued from these scenarios. The calculations presented in this report have been based on these data.

Emissions scenarios have undergone some revisions since October 2010, mainly to respond to requests from the Working Group on Strategy and Review (WGSR). It is therefore expected that an update of this work will be carried out in the summer/autumn 2011 to ensure a close correlation to the emission scenarios that will be used in the latest stage of the Gothenburg protocol revision (expected at the end of 2011 or early 2012).

2.2 FURTHER SCENARIOS DEVELOPED BY THE TF IAM

In this report, only results for the historical situation and baseline and MFR projections are presented. The WGSR requested that CIAM investigated the consequences of "hybrid" scenarios: These illustrate situations intermediate between the current legislation based baseline scenario and the "all feasible technology reductions" MFR scenario. Such scenarios were not made available at the time of gathering information for this report and therefore are not discussed here.

In a second exercise, to be carried out in the second half of 2011, new scenarios may be analysed, following the approach described below.

This interim report gives nevertheless a robust indication of the range of the results that will be obtained when definite scenarios will be available. Absolute values of figures will change but not their order of magnitude nor will the trends presented and discussed here.

3. ICPS AND TASK FORCE RESULTS

3.1 ICP FORESTS

On 107 ICP Forests Level II sites, located in 17 countries, throughfall N and S depositions were measured and deposition of base cations was estimated. Following the steady-state simple mass balance (SMB) approach (UBA, 2004), based on soil, soil solution and deposition data, critical load functions and their exceedances were calculated on each of these sites using either ICP Forests measured throughfall deposition, modelled EMEP deposition (for the year 1980) and the "2010 deposition datasets".

The VSD+ model was applied to 77 ICP Forests sites. VSD+ is an extension of the steady-state Simple Mass Balance model into a dynamic soil model by including cation exchange (with the Gaines-Thomas or Gapon relationships) and time-dependent N immobilisation. It is especially designed for use on a site specific scale and in support of the review of effects-based Protocols under the LRTAP Convention (Bonten et al., 2009).

Results of the SMB method suggest that in 1980 the critical loads for acidity were exceeded on all plots in central Europe (Figure 2a). At the same time, no exceedances were observed on calcareous soils (i.e. on many Mediterranean sites) nor where deposition was low (like in Scandinavia). Since then, the situation is shown to be improving. Calculations suggested that in 2000 there were no exceedances on more than 80%. Further improvements are forecasted with the three 2020 projections, with the MFR scenario leading to widespread non exceedances. A comparison with critical load for acidity calculated with measured throughfall deposition (Figure 2f) reveals an intermediary situation between 2000 and 2020, even though the number of observation plots is not fully comparable.

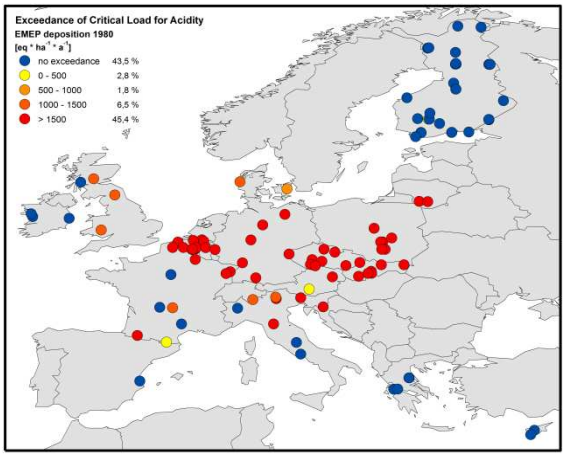

Figure 2a

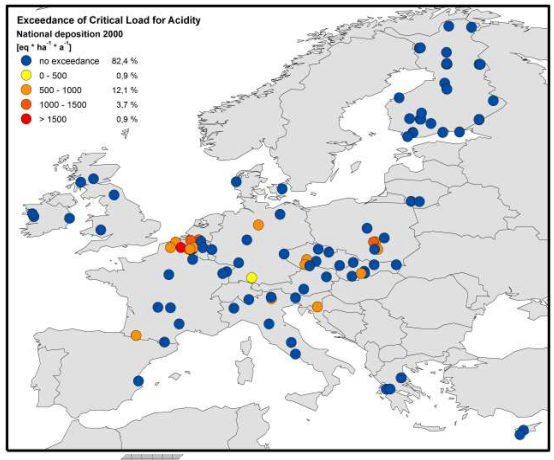

Figure 2b

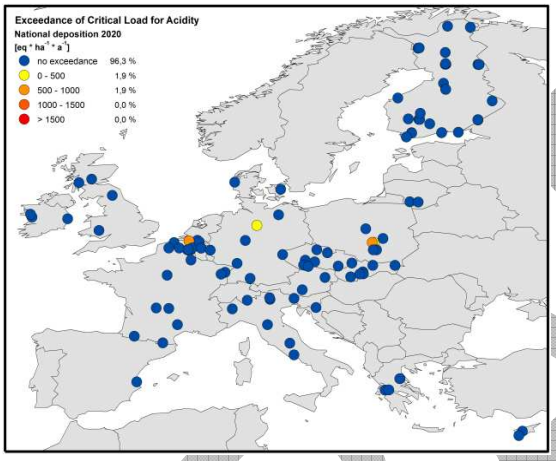

Figure 2c

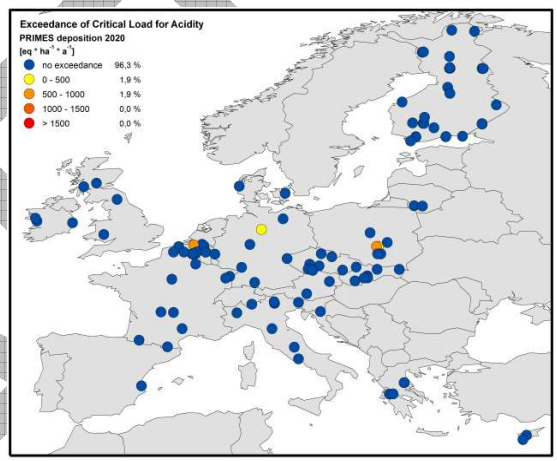

Figure 2d

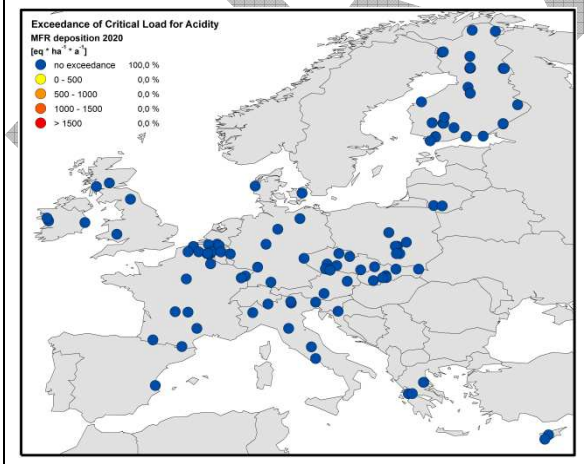

Figure 2e

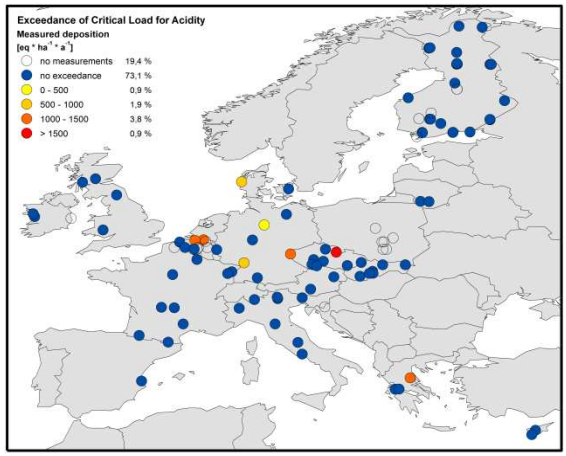

Figure 2f

Figure 3: Exceedances of critical loads for acidity in the years 1980(a), 2000(b), and 2020 national projection (c), modelled by PRIMES (d), MFR scenario (e), and exceedance of critical loads by the latest known ICP Forests throughfall measurements (f)

In 1980, critical loads for nutrient nitrogen were exceeded on about 60 % of the plots (Figure 3a). The high exceedance of the critical loads implies a high risk of eutrophication for the forest ecosystems. Most plots in the centre of Europe, in the United Kingdom, in southern France, in Northern Italy and in Spain were affected.

Even though the exceedances were mostly lower in 2000, the share of plots with exceedances hardly decreased over two decades. The NAT2020 and the PRI2020 projections show similar results for the year 2020, i.e. a further decrease of the number of sites with exceedances to approx. 30% of the plots. Maximum technically feasible reductions (MFR) would improve the situation, but still would not protect all sites from eutrophication risks.

The dynamic model VSD+ was run on 77 plots across Europe with future depositions according to the NAT2020 projection (Figures 4 to 6).

Statistical analysis of the model results suggests that most changes in the plots base saturation condition occurred between the years 1960 and 2000 (Figure 5). The share of plots in the "<20%" class doubles between 1980 and 2000, at the expense of the number of plots with a base saturation between 20 and 40%. After 2000, the model predicts hardly any changes on more than 90% of the plots. Model runs over longer time periods give similar results.

A complementary analysis shows that the spatial trend for base saturation in soil solution of different plots is heterogeneous although there is a tendency towards low base saturation for central and eastern/north-eastern Europe in all years where acidification has been the most intense.

Soil pH hardly shows any spatial trend. Statistical analysis indicates that major changes occurred between 1950 and 2000 (Figure 6). These changes include an increase in the share of plots with extremely low pH values in the 1970s and 1980s and a recovery from 1990 onwards. This suggests a strong link with the SO_2 peak emissions shown on Figure 2. Between the years 2000 and 2050, there is no significant change visible on 93% of the plots.

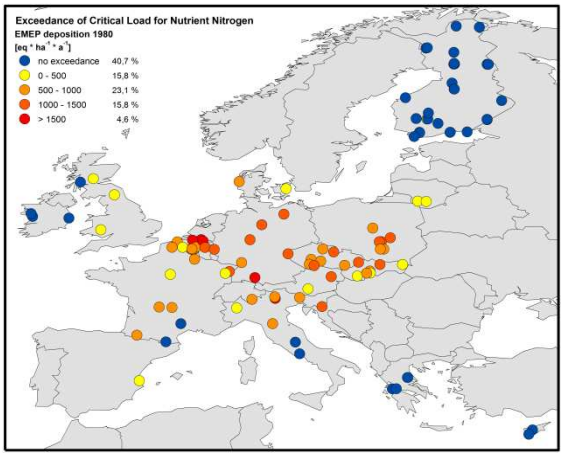

Figure 3a

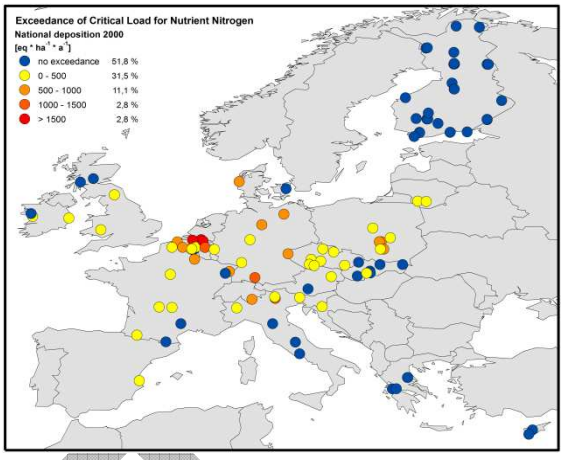

Figure 3b

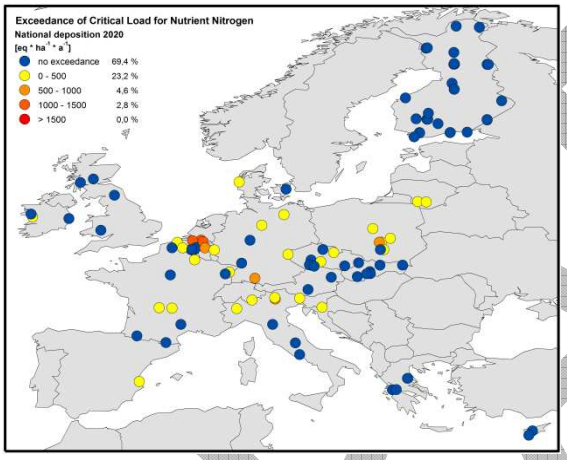

Figure 3c

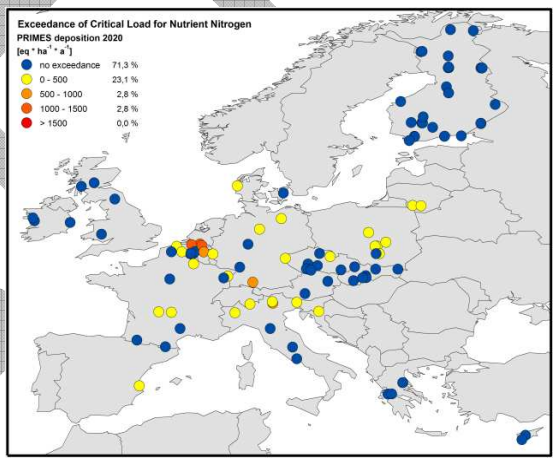

Figure 3d

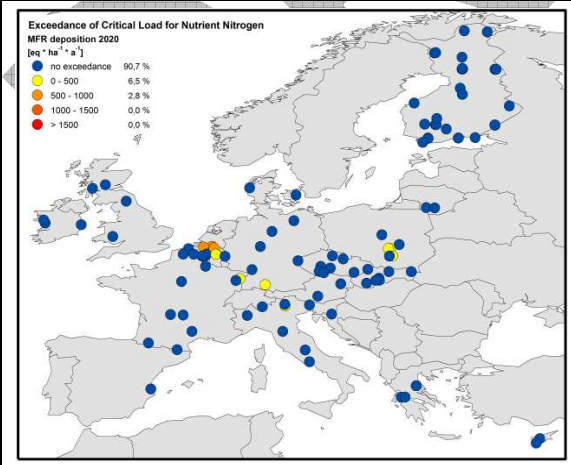

Figure 3e

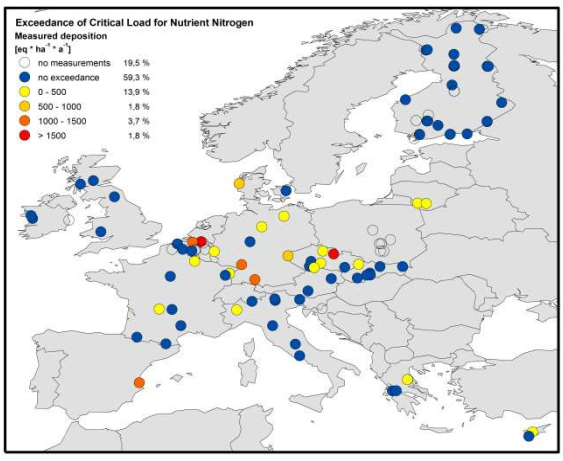

Figure 3f

Figure 4: The exceedance of critical loads for nutrient nitrogen in the years 1980(a), 2000(b), 2020 national projection (c), modelled by PRIMES (d), MFR scenario (e) and the latest known ICP Forests throughfall measurements (f)

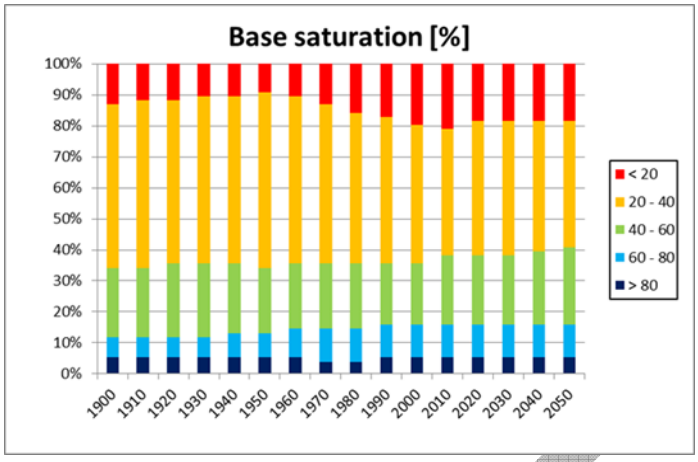

Figure 5: Overall trend for base saturation classes modeled by VSD+

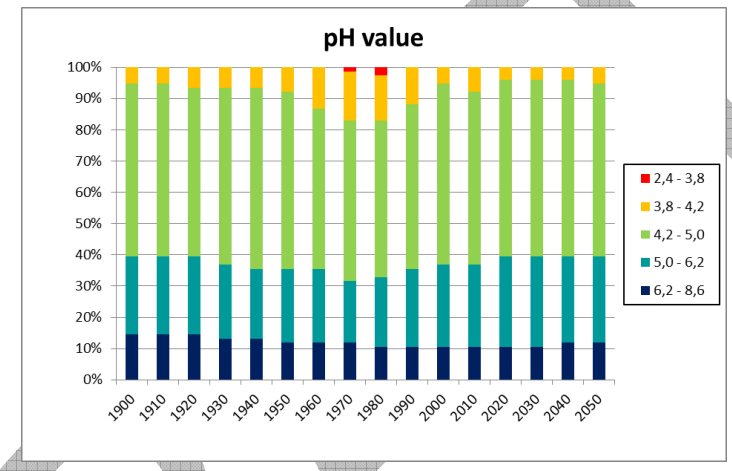

Figure 6: Overall trend for pH value modelled by VSD+ and classified by buffering classes (Ulrich 1981).

The model results for the C:N ratio suggest that in the year 1950, about 40 % of the plots were characterized by mesotrophic conditions with a C:N ratio between 18-24 (Figure 7). Altogether, about 80% of the plots were calculated to be either in mesotrophic conditions or oligotrophic (C:N>24). The number of plots with eutrophic conditions (C:N<17) was calculated to increase continuously since 1950. Their share reached 40% of the plots in 2000. This eutrophying trend is calculated to continue until 2050 when eutrophic conditions will dominate. Hypertrophic conditions (C:N<10) are predicted for a small share of plots in the second half of the modelled period.

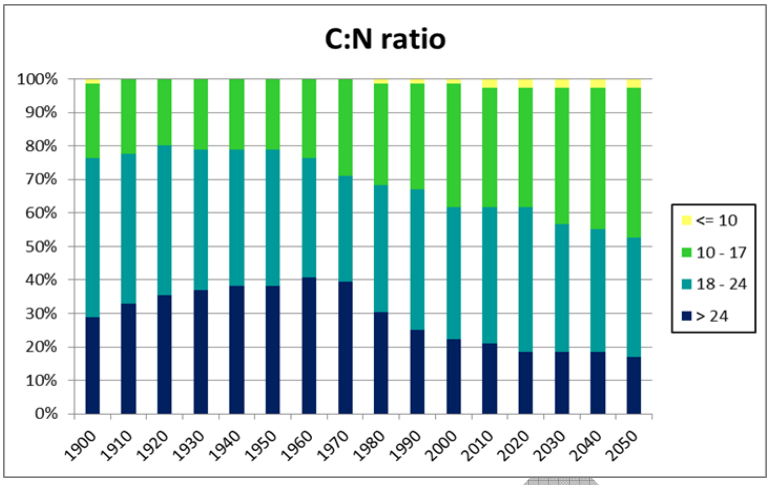

Figure 7: Overall trend for C:N ratio modelled by VSD+ and classified by nutrient levels.

3.2 ICP WATERS

ICP Waters assessed the effects of the deposition projections by means of the dynamic biogeochemical model MAGIC (Cosby et al. 1985, 2001). In the past, MAGIC has been extensively used to assess soil and water acidification, including a major assessment of the implementation of the Gothenburg protocol (Wright et al. 2005). MAGIC provides an estimate of surface water acidification status (as indicated by the acid neutralising capacity; ANC) in response to a given scenario of S and N deposition over time.

The resulting estimates of ANC were then used to evaluate biological response. There are robust dose-response relationships between ANC and key indicators of ecosystem damage, such as viable population of fish (brown trout, salmon), biodiversity of groups such as diatoms, invertebrates, and aquatic plants. These indicator organisms have been used to set critical limits (ANC_{limit}), which in turn have been used to determine critical loads of acidity (CL_A) (Henriksen and Posch, 2001).

Lake Saudlandsvatn, southern Norway, provides a 35-year record that illustrates the rise and fall of acid deposition, acidification of water and damage and recovery to key biota (Hesthagen et al. in prep.).

At the start of the monitoring in 1974 the non-marine S deposition (S*) greatly exceeded the critical load for acidity, the lake was acidified and had negative ANC (far below the ANClimit) and low pH (around 5 which is significantly much below natural background level of 5.5 – 6.0 from a biological point of view). Short-lived biological acid-sensitive indicator organisms (invertebrates and zooplankton) were absent and the native brown trout population was on its way to extinction. Since about 1988, S* deposition has decreased sharply (Figure 2), ANC and pH have increased and starting in the late 1990s the biota has begun to recover (Figure 8).

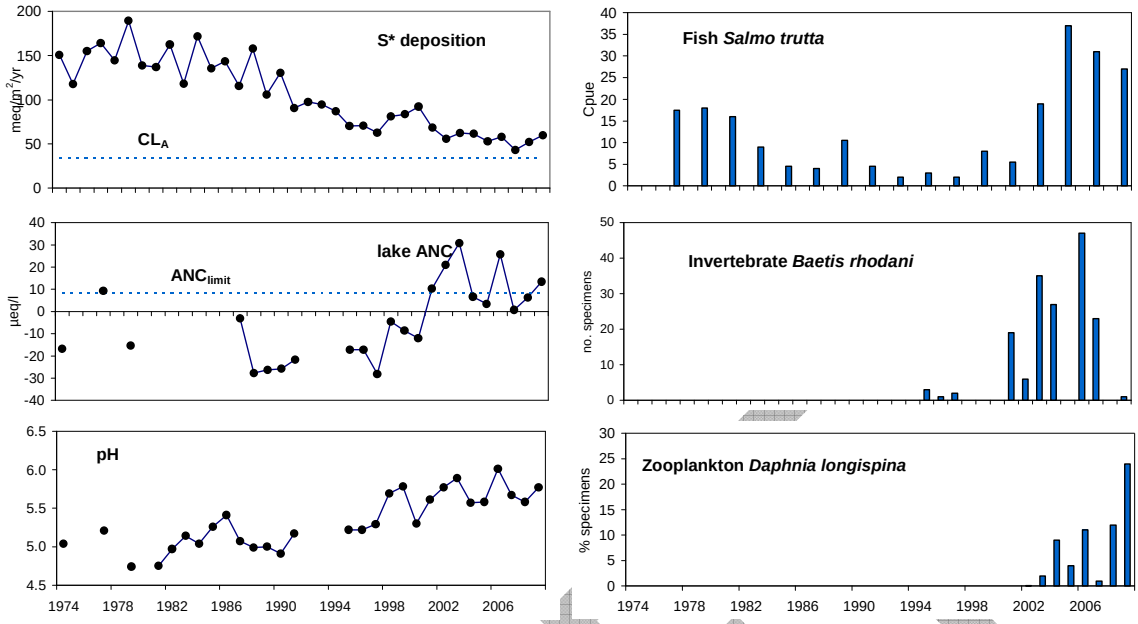

Figure 8: Long-term deposition, lake chemistry and lake biology monitoring data for Lake Saudlandsvatn, an ICP Waters site in southern Norway. Shown are non-marine S (S) deposition, lake ANC and pH, catch-per-unit effort of fish, number of specimens collected of the acid-sensitive mayfly B. rhodani, and % specimens collected of the acid-sensitive zooplankton species D. Longispina (Data from Hesthagen et al. 2011).*

At Lake Saudlandsvatn more than 90% of deposited N is retained in the lake and catchment and this situation has not changed during the 35 years of monitoring. Nitrogen deposition does not greatly affect lake acidification at least at present. Modelling focus can thus be placed on S* deposition.

MAGIC was first calibrated to the observed annual water chemistry data from the 1974-2009 period and driven by the historical S and N deposition data for the EMEP grid square 50-57 provided by the CCE in the 2007/8 call (see insert for explanation on the CCE 2007/8 call). The deposition specified by the projection NAT2000 was scaled to the measured deposition at the site for the year 2000. The calibrated parameter set was then run with scenarios for future deposition of S and N (projections NAT2020, PRI2020 and 2030, and MFR2020).

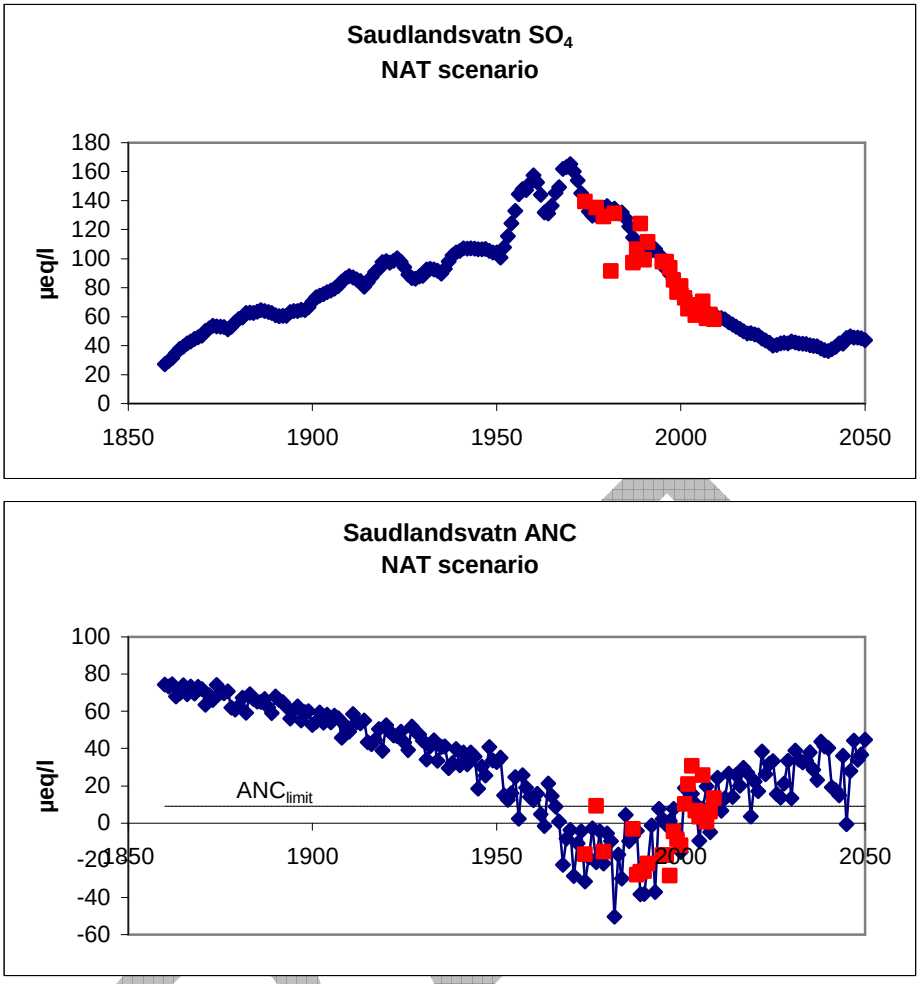

Figure 9: Concentrations of sulphate (SO_4) and ANC in Lake Saudlandsvatn measured (red squares) and simulated (blue diamonds) with the MAGIC model. The future simulated values assume S deposition as specified by the NAT scenario for 2000 and 2020, and constant level past the year 2020.*

The long-term reconstructed acidification history at Lake Saudlandsvatn suggests that ANC fell below the ANC_{limit} for fish around 1950 and that ANC remained well below the ANC_{limit} until recently (Figure 9). The year-to-year "noise" in ANC with present-day amplitude of about 30 µeq/l reflects natural variations in amounts of precipitation and seasalt inputs.

With the NAT projections, ANC levels are expected to continue to increase somewhat over the next 10 years, and then level off at about ANC 30 µeq/l. Year-to-year fluctuations, however, imply that ANC will fall below ANClimit during "bad" years, years with high seasalt inputs (Figure 9).

The projected ANC for the year 2020 was almost the same with the three 2020 projections, with additional improvements given the MFR2020 projection (Figure 10). This is because the future S* deposition is very similar under NAT 2020 and PRI2020 and somewhat less under MFR2020.

Remark on deposition data from various sources

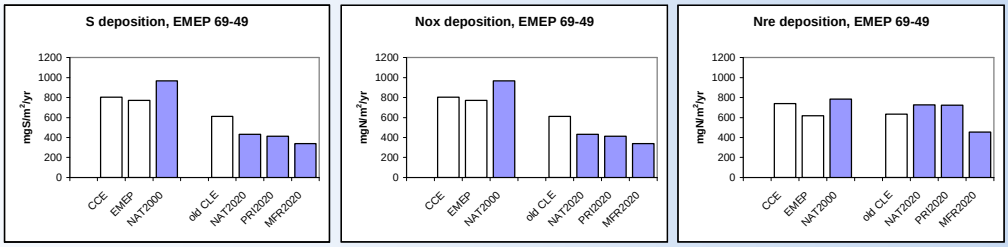

An example of deposition scenarios for S, N oxidised, and N reduced, here shown for the EMEP grid square 69-49 (Czech Republic). Shown are data supplied by the CCE in the 2007/8 call for the year 2000 (labelled "CCE") and projected for the year 2020 under the current legislation scenario (labelled "old CLE") and data for the scenarios NAT2020, PRI2020 and MFR2020. Also given are the modelled EMEP deposition values for the year 2000 (labelled "EMEP).

The deposition data for the NAT 2000 scenario differ from the values for the year 2000 supplied by the CCE in the 2007/8 call and both these differ from the modelled EMEP deposition for the year 2000 (Figure aa). ICP Waters had previously used the data supplied in 2007/8 to carry out dynamic modelling at many monitoring sites. These dynamic modelling calibrations and results for the 14 scenarios stipulated by the CCE in the 2007/8 call formed part of the responses by the national focal centres to the 2007/8 call for data. These data are used here by the CCE to present Europe-wide assessments of the three new scenarios for the year 2020.

As acidification of soil and water and the recovery at any given time is a function of the total cumulative acid deposition since the onset of acid deposition, changing estimated deposition of the calibration year means that the calibration must be done anew. ICP-W chose to use the calibrations from the 2007/8 call. The NAT2000 data were thus downscaled to the values for 2000 CCE 2007/8. This means that the reconstruction of acidification history at the various sites is not affected.

The differences between deposition data as calculated by EMEP models has varied between the years, partly because emissions estimates have been modified by parties and by including new data, partly because EMEP modelling has been improved to take into account additional processes, and partly because EMEP results have been linearised to accelerate calculations and to make possible to provide results for more scenarios.

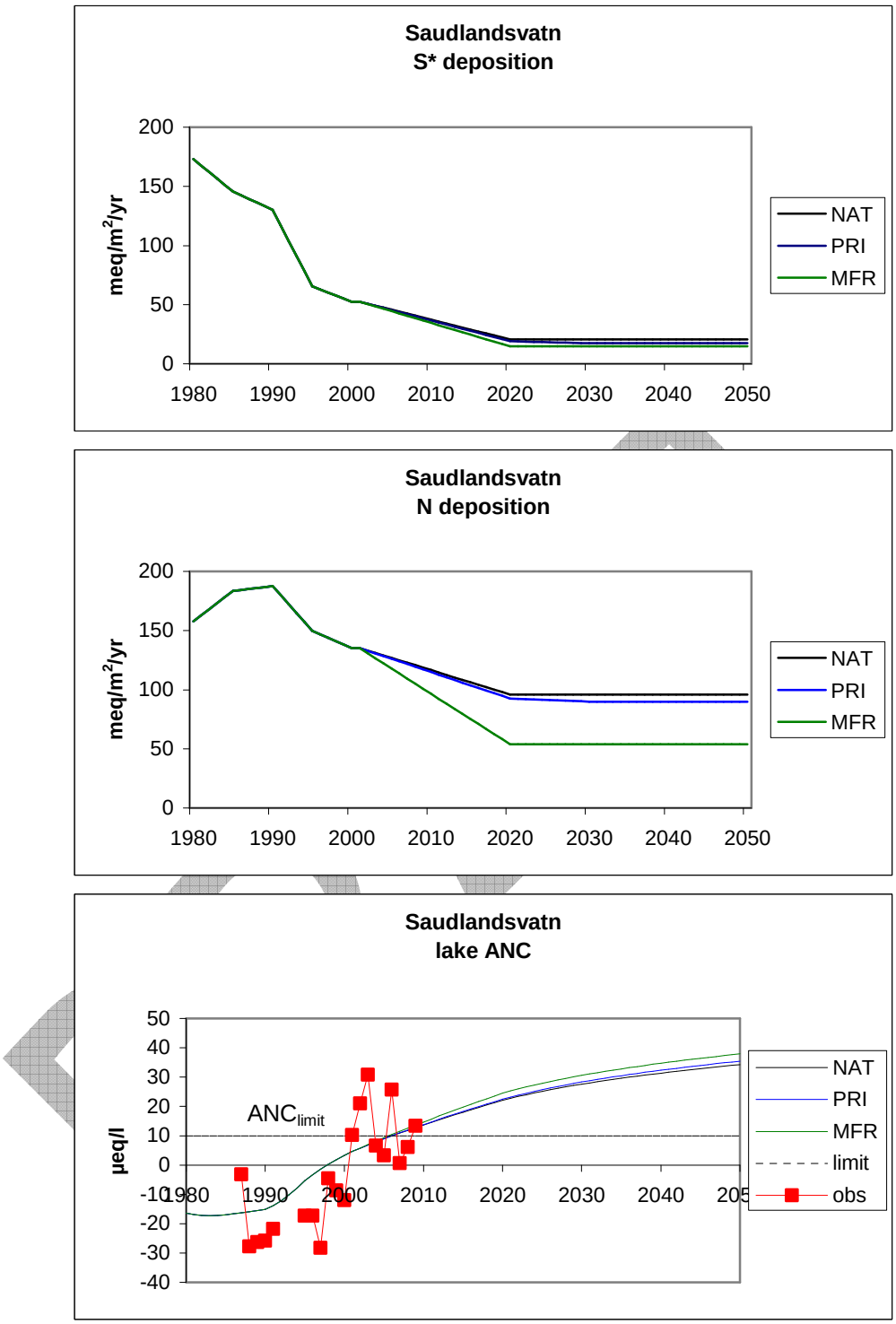

Figure 10: Non-marine S and N (oxidised and reduced) deposition scenarios used to drive the MAGIC model and the resulting ANC projections at the Lake Saudlandsvatn, southern Norway. Also shown are the annual observed ANC concentrations (red squares) and the ANC_{limit} for brown trout in the lake (dashed line).

The same procedure was used to calibrate and run MAGIC with the scenarios at 10 acid-sensitive lakes in Europe (Figure 11, Table 1). These lakes are monitored as part of ICP Waters network.

Table 1: Locations of ICP Waters sites used for the assessment of the different projections.

SITE	COUN-TRY	LAT N	LONG W	EMEPi	EMEPj	GRID-CODE	REFERENCE
Lake Paione Superiore LPS	IT	46.1739	8.1908	70	37	70-37	Rogora 2004
Round Loch GH	UK	55.0833	-4.4167	43	44	43-44	
Grannoch	UK	55.0000	-4.2667	43	44	43-44	
Cerne	CZ	48.9667	13.5000	71	48	71-48	
Lysina	CZ	50.0500	12.6667	69	49	69-49	
Maly Staw	PL	50.7486	15.7006	71	53	71-53	
Długi Staw	PL	49.2267	20.0089	78	56	78-56	
Saudlandsvatn	NO	58.2000	6.7667	50	57	50-57	Hesthagen et al. 2001.
Lille Hovvatn	NO	58.6000	8.0167	51	59	51-59	Hindar and Wright 2005

Figure 11: Map of Europe showing the location of the 9 ICP Waters sites used with the MAGIC model for the present assessment.

The results (Figure 12 and Table 2) indicate that at all sites the future S and N deposition described by the NAT, PRI and MFR projections will result in substantial improvement in water quality. Whether the lakes will fully recover both chemically and biologically depends, of course, on the degree of acid sensitivity of the site. For example, under NAT2020 scenario, recovery at Lake Saudlandsavatn can be expected whereas at Lake Lille Hovvatn the remaining acid deposition will cause sufficient acidification for the lake ANC to lie below the critical limit (ANClimit), which implies that key indicator organisms such as fish will not fully recover.

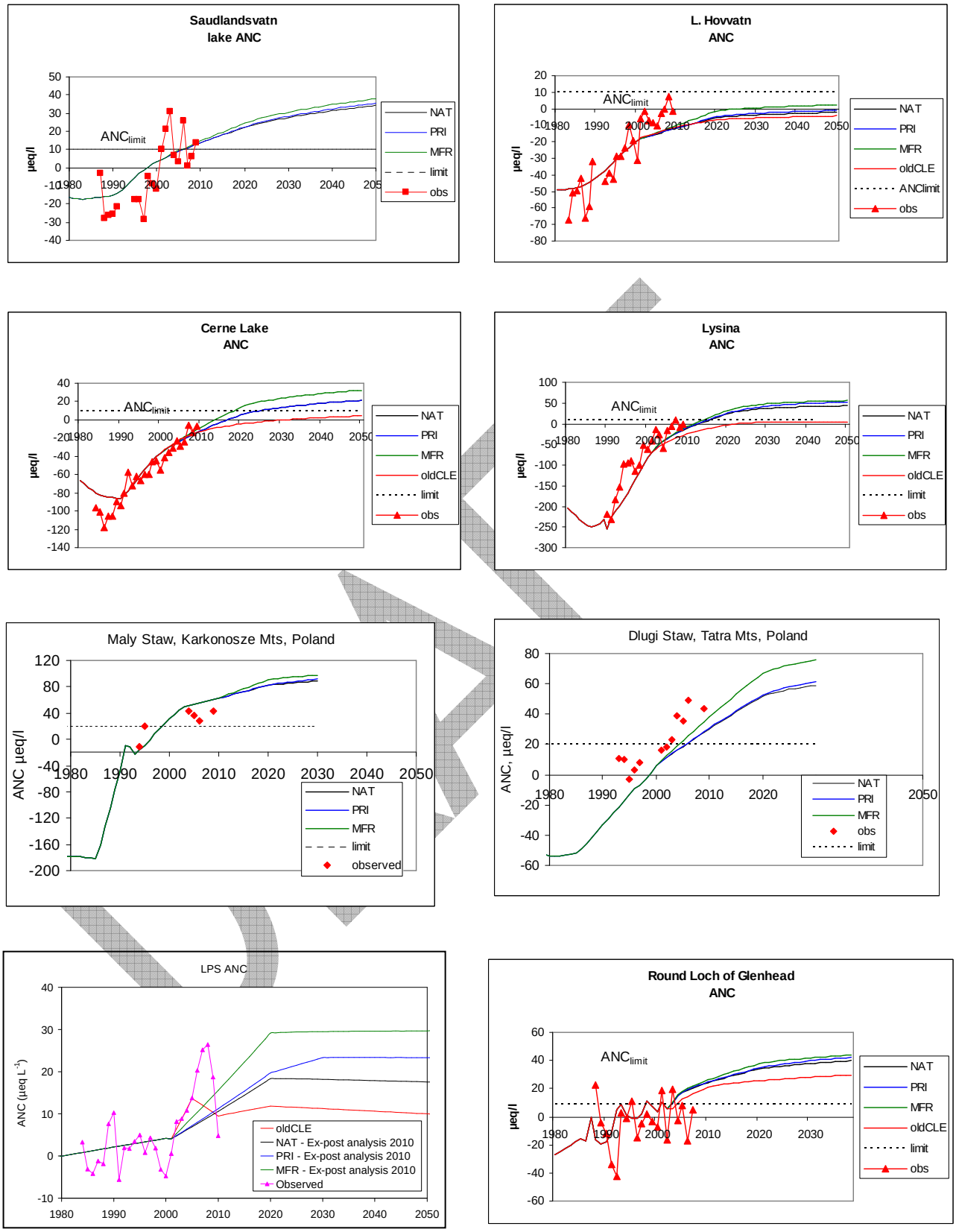

Figure 12: ANC concentrations at ICP Waters sites in Europe as simulated by MAGIC under several scenarios of future S and N deposition (lines). Observed depositions are shown (red squares). See Table 1 for site details.

*Table 2: Summary of biological status in the study lakes observed (1990, 2000, 2010) and forecast recovery under the old CLE and ex-post scenarios. Recovery classes: 0 no recovery; * start recovery; ** partial recovery; *** full recovery. Organism groups: f = fish; zp = zooplankton; zb = zoobenthos; dia = diatoms. NS: not significant.*

	Status 1980	Status 2000	Status 2010	Forecast 2020 old CLE	Forecast 2020 NAT=PRI	Forecast 2020 MFR	Forecast 2030 PRI	Organism group
LPS	0	0	0	0	**	***	**	zb, dia
Round	0	0	*	***	***	***	***	f, zb, dia
Cerne	0	*	*	**	**	***	***	zp, zb
Lysina	0	0	*	**	***	***	***	zb
Maly	0	NS	NS	NS	***	***	***	zp, dia
Dlugi	0	0	NS	NS	***	***	***	dia
Saud	0	*	**	**	***	***	***	f, dia
L. Hov	0	0	0	0	0	0	0	f, dia

3.3 ICP INTEGRATED MONITORING

3.3.1 ASSESSMENTS OF CRITICAL LOADS AT ICP IM SITES

Critical loads for acidification CL_A, mass balance calculated critical load of nutrient nitrogen $CL_{nut}N$ and empirical critical loads for nutrient nitrogen $CL_{emp}N$ were evaluated at ICP Integrated Monitoring (IM) sites. Exceedance of critical loads were estimated for the baseline (NAT2000 and NAT2020, PRI2020 and PRI2030) and Maximum Feasible Reduction (MFR2020) scenarios. Modelled deposition for 1995 were obtained from EMEP (EMEP WebDab 2010) as grid average values. Furthermore, the relationships between present exceedances of critical loads of acidification and eutrophication for terrestrial and aquatic ecosystems (using NAT2000 deposition scenario) and empirical surface water chemistry results were studied. The collected empirical data of the ICP IM was used for testing/validating the key concepts in the critical load calculations and for assessing the confidence in the regional scale critical loads mapping approach used in the integrated assessment modelling.

Critical loads for acidification (CL_A) of aquatic ecosystems were calculated for 14 IM sites, for which observations of runoff volume and water chemistry were available. The Steady-State Water Chemistry (SSWC) model was used (Henriksen and Posch, 2001, UBA, 2004).

Critical loads for eutrophication of terrestrial ecosystems were calculated for mass balance critical load of nutrient nitrogen ($CL_{nut}N$) and for empirical critical loads for nutrient nitrogen ($CL_{emp}N$). Mass balance critical loads for nutrient nitrogen $CL_{nut}N$ were calculated with a nitrogen budget equation for the same 14 IM sites for which observations of runoff volume were available, with the addition of information for one site. Details of the calculations may be found in Holmberg et al. (2009).

The empirical critical loads of nitrogen were compiled for another 24 sites in addition to those mentioned above. This analysis was based on reported critical loads of nutrient nitrogen from extensive empirical studies on the response of terrestrial ecosystems to nitrogen deposition (Achermann and Bobbink, 2003).

Calculations with the MFR2020 deposition reduced the average exceedance of CL_A for aquatic ecosystems (Table 3) and increased the number of ICP IM sites protected from 9 to 12. However, due to the sensitivity of the sites, even the MFR2020 scenario would not protect all the sites.

Table 3: Average exceedance of critical loads of acidification CL_A (eq/ha/yr) and eutrophication CLnutN and CLempN (eq/ha/yr and kg/ha/yr). 1995: Deposition modelled by EMEP. Future deposition estimates according to the NAT2000, NAT2020, PRI2020, PRI2030 and MFR2020 datasets.

Average exceedance	1995	NAT 2000	NAT 2020	PRI 2020	PRI 2030	MFR 2020	Nr of sites or plots in calculations
CL_A (eq $ha^{-1}yr^{-1}$)	196	73	7.3	6.1	2.9	1.5	14 sites
CLnutN . (eq $ha^{-1}yr^{-1}$)	440	530	340	320	210	110	15 sites
(kg $ha^{-1}yr^{-1}$)	*6.1*	*7.4*	*4.7*	*4.5*	*4.1*	*1.5*	
CLempN (eq $ha^{-1}yr^{-1}$)	190	340	140	140	110	70	85 plots on 37 sites
(kg $ha^{-1}yr^{-1}$)	*2.6*	*4.8*	*2.0*	*1.9*	*1.5*	*0.1*	

Regarding the critical loads for eutrophication for terrestrial ecosystems ($CL_{nut}N$ and $CL_{emp}N$) only the MFR2020 scenario would significantly reduce the average exceedance of critical loads and protect most of the plots in the ICP IM sites (Figure 13 and Table 3).

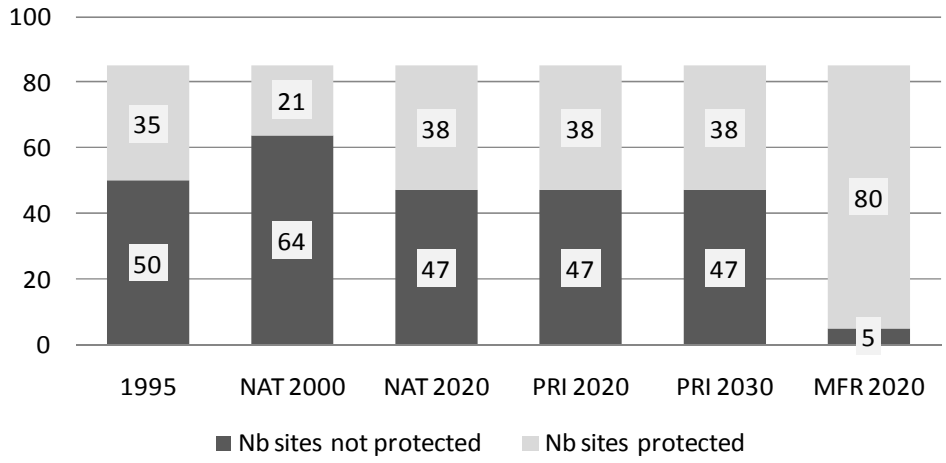

Figure 13: Number of plots in ICP IM sites that are protected/not protected for eutrophication (according to calculations based on empirical critical loads) assuming different deposition scenarios.

3.3.2 COMPARISON OF EXCEEDANCE OF CRITICAL LOADS WITH EMPIRICAL EFFECTS INDICATORS

The collected empirical data of the ICP IM allows testing/validation of the regional scale critical loads mapping approach used in the integrated assessment modelling. The comparison between empirical observations and critical thresholds was done for 14, 15 or 24 IM sites, depending on availability of empirical monitoring data. The relationship between exceedance of CL_A (using NAT2000 deposition scenario) and empirical observations was expressed for a selection of 14 sites, for which observations of runoff volume and runoff water chemistry were available. Correspondingly for the exceedance of $CL_{nut}N$, same 14 IM sites were used with the addition of information for site AT01. The relationship between exceedance of $CL_{emp}N$ and empirical observations was expressed for 24 sites.

In order to compare the effects with exceedances of critical loads at IM sites (using NAT2000 deposition scenario), the median annual runoff water fluxes and concentrations of key acidification parameters (ANC, H^+ and SO_4) and nutrient nitrate-nitrogen (NO_3) for the period 2002-2006 were used as empirical impact indicators (Vuorenmaa et al., 2009). Runoff water fluxes were calculated from the quality and quantity of water using mean monthly values for water fluxes and chemical analyses.

There was a good agreement between exceedance of critical load for acidification (CL_A) and empirical acidification indicators in runoff water both in median annual fluxes and concentrations (Figure 13). At the most acidified or acid sensitive sites (in terms of low ANC and high H^+ concentrations and fluxes), the sulphur deposition exceeded critical loads for acidification to a higher degree than at other sites. Correlation between sulphate and CL_A exceedances among the IM sites was poorer, due to differences in soil susceptibility to acidification. Some sites are located in calcareous soil with high initial concentrations of sulphate and calcium and magnesium, and high concentrations of ANC, and are therefore well protected against acidification. At the sensitive sites, the quantitative estimate for negative exceedance of critical for acidification (i.e. no-exceedance) is lower, or $ExCL_A$ is increasing with increasing sulphate flux.

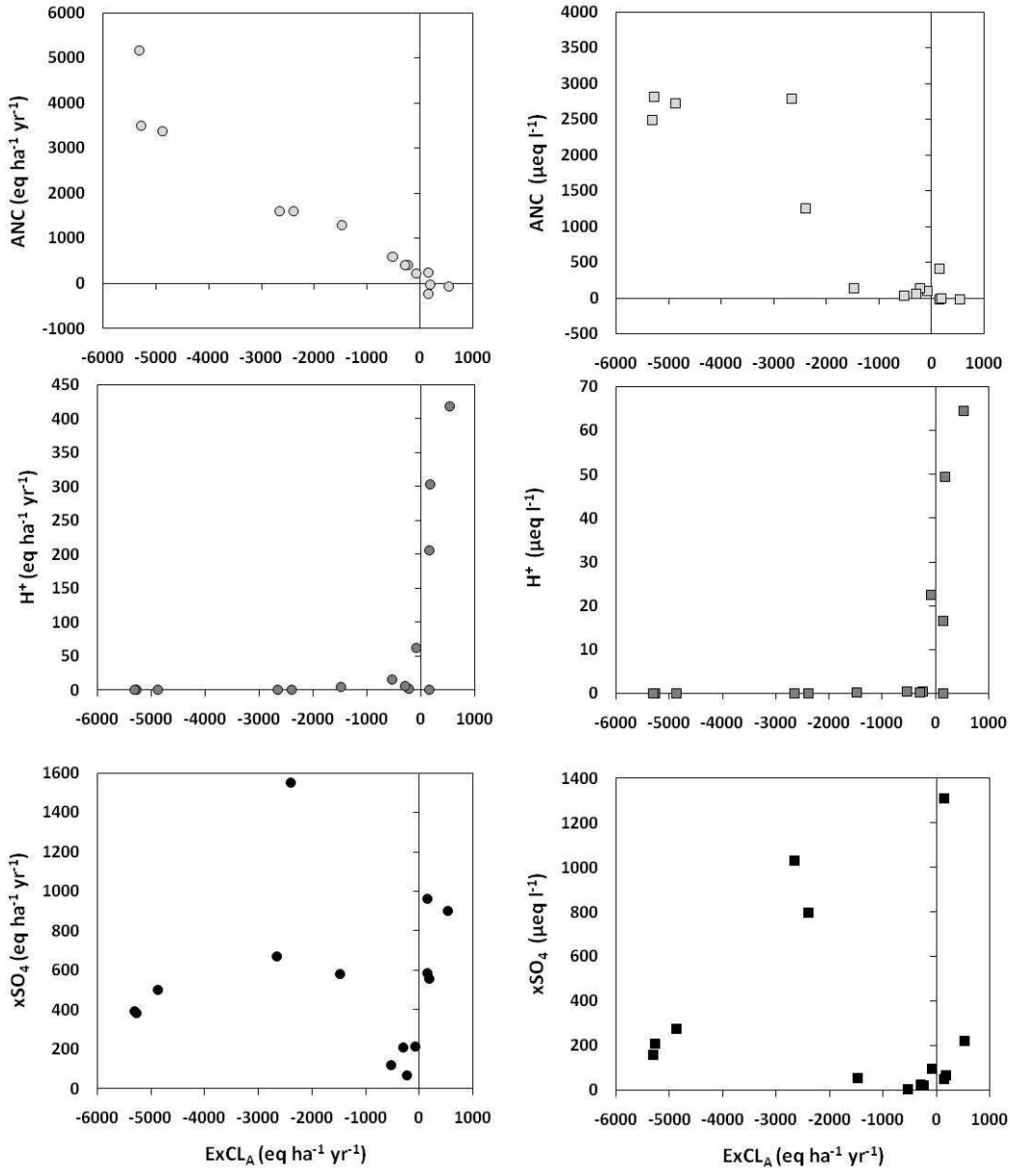

Figure 14: Exceedance of critical load for acidification ($ExCL_A$, eq ha^{-1} yr^{-1}, NAT2000 scenario, x-axis) for aquatic ecosystems vs. annual median fluxes (left column) and concentrations (right column) measured between 2002 and 2006 (y-axis) of ANC, H^+ and non-marine sulphate (xSO_4) in runoff for 14 ICP IM sites. Negative exceedance values are included in graphs in order to show the difference between deposition and critical load value, also in the case that CL is greater than deposition.

There was also evidence that the sites in which empirical critical load of nutrient nitrogen for terrestrial ecosystems ($CL_{emp}N$) was exceeded, exhibited also higher nitrate concentrations and fluxes in runoff. Correspondingly, the leaching of nitrate increased with increasing critical load exceedance of mass balance nutrient nitrogen ($CL_{nut}N$, Figure 14).

These observations give evidence on links between modelled critical thresholds and empirical results for acidification parameters and nutrient nitrogen.

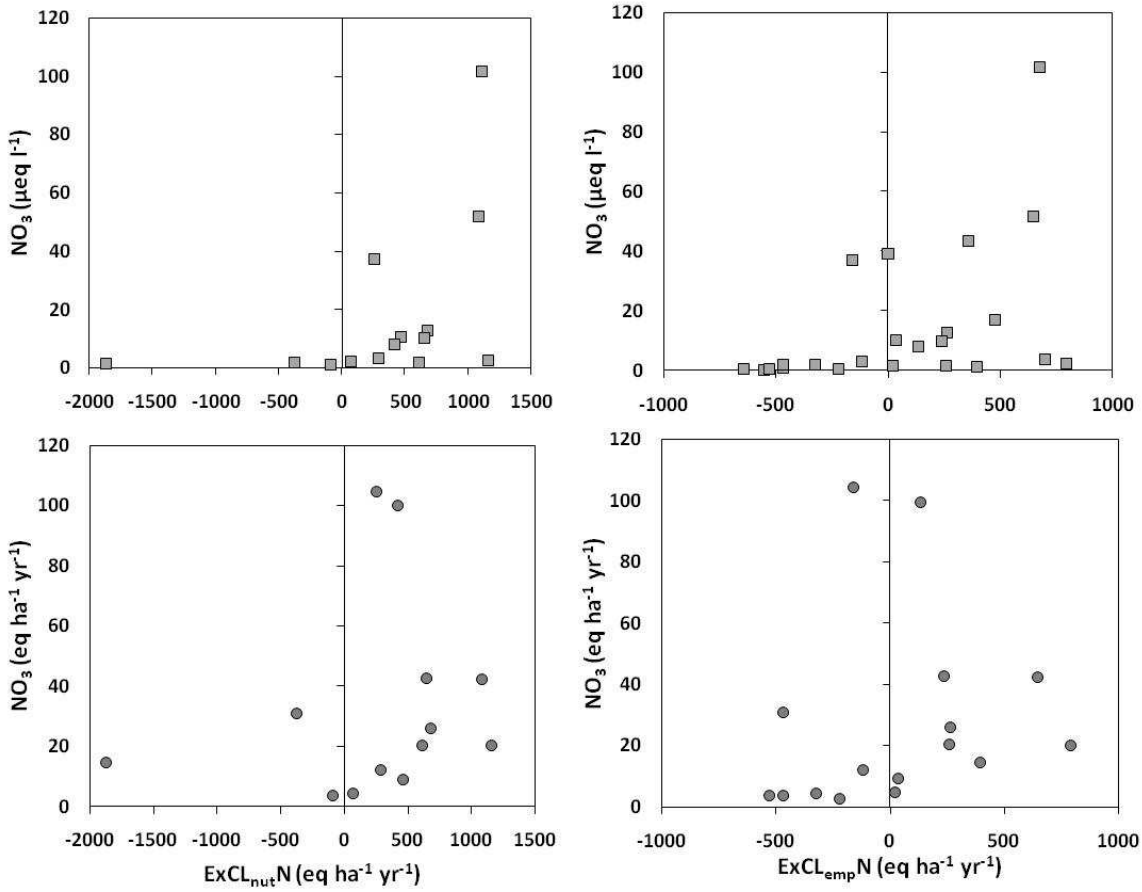

Figure 15: Exceedance of critical load for mass balance nutrient nitrogen ($ExCL_{nut}N$, eq ha^{-1} yr^{-1}) (x-axis) vs. median annual fluxes (left down) and concentration (left upper) (2002-2006) (y-axis) of NO3 in runoff for 13-20 ICP IM sites, and exceedance of empirical values of critical load for nutrient nitrogen ($ExCL_{emp}N$, eq ha^{-1} yr^{-1}) (x-axis) vs. median annual fluxes (right down) and concentrations (right up) (2002-2006) (y-axis) of NO3 in runoff for 16-23 ICP IM sites. Exceedance values were calculated using the NAT2000 deposition scenario. Negative exceedance values are included in graphs in order to show the difference between deposition and critical load value, also in the case that CL is greater than deposition.

3.4 ICP MODELLING AND MAPPING

3.4.1 ACCUMULATED AVERAGE EXCEEDANCES AND AREA AT RISK OF ACIDIFICATION AND EUTROPHICATION

ICP Modelling and mapping (ICP M&M) provide an European wide assessment of critical loads for acidification and eutrophication and of their exceedances. Results Are presented either as tables or as maps (Figures 15 and 16). Tables lists the percentage of a country's natural area that is at risk due to exceedance of critical loads of acidification or eutrophication, as well as the magnitudes of the Average Accumulated Exceedance for each country. Here, only values for the EU27 and the whole EMEP area are shown (Table 4). Full results are to be found in Hettelingh et al. (2011). Maps illustrate the location and magnitude of these areas in each EMEP grid cell. Finally, tentative results are described of areas where the change of biodiversity caused by excessive N-deposition is significant, i.e.

exceeds 5%. Compared to earlier CCE reports, a new indicator “environmental improvement” is introduced to mark scenario specific progress in time.

The environmental improvements between 2000 and 2020 are visible in two ways. Maps (Figure 16 and Figure 17) indicate where and by how much accumulated average exceedances are modified as N and S depositions decrease. Tables 4 to 7 (Table 4,

Table 5, Table 6, Table 7) provide this information in more quantitative terms at the European scale (whole Europe and EU27).

In 2000, areas at risk of acidification were smaller than areas at risk of eutrophication. Under the MFR scenario and to a lesser extend to the baseline scenario, calculations indicate clear decrease of the areas at risk for both acidification and eutrophication by 2020. This is illustrated by the decrease of the coloured cells on the maps (Figure 16 and Figure 17). A quantitative evaluation of the concerned areas is also given in Table 4. It shows that for acidification improvement occurs on 6% of the whole Europe with the baseline scenario (NAT2020) and on 9% with the MFR scenario. For eutrophication, environmental improvement concerns 14% of the whole Europe with the baseline scenario and 38% with the MFR scenario.

Table 4: Evolution of the areas at risk of acidification and eutrophication in Europe according to the scenarios baseline (NAT) and MFR. All % refer to the whole EU27 or European areas.

% area at risk		**NAT2000**	**NAT2020**	**MFR2020**
EU27	Acidification	19%	4%	2%
	eutrophication	74%	61%	24%
Europe	Acidification	10%	4%	1%
	eutrophication	52%	38%	14%

The magnitude of the risk is also expected to diminish between 2000 and 2020. On Figures 15 and 16 (Figure 16 and Figure 17), this is shown by the lesser occurrence of cells in red and yellow. Thus, countries with areas suffering from the highest exceedances of critical loads for nitrogen (> 1200 eq $ha^{-1}yr^{-1}$) in 2000, such as in western France, along the border-area between Germany and the Netherlands, in Denmark and in northern Italy, clearly benefit from reductions computed for 2020 under both the baseline and maximum feasible reductions scenarios. In some countries (Czech Republic, Denmark, Hungary, Liechtenstein, Lithuania, Macedonia, Slovakia and the Ukraine) the area at risk does not change between 2000 and 2020. However, in these countries, the magnitude of the excess decreases significantly too.

Table 5 summarise this point for EU27 countries and the whole Europe.

Environmental improvement for accumulated average exceedance (AAE) is calculated as a % of reduction. For acidification, environmental improvement occurs on 78% of the whole Europe with the baseline scenario NAT2020 and 96% with the MFR scenario. For eutrophication, environmental improvement over Europe is 45% and 90% for NAT2020 and MFR2020 respectively.

Table 5: Evolution of the Accumulated Average Exceedance of critical loads for acidification and eutrophication (eq ha^{-1} yr^{-1}) in Europe according to the baseline (NAT) and MFR scenarios.

AAE (eq ha^{-1} an^{-1})		**NAT2000**	**NAT2020**	**MFR2020**
EU27	Acidification	108	24	4
	Eutrophication	333	179	35
Europe	Acidification	54	12	2
	Eutrophication	185	102	18

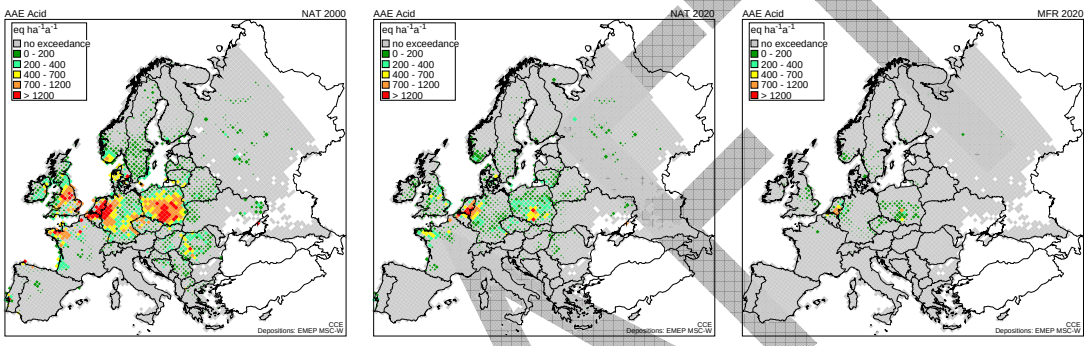

Figure 16: Average Accumulated Exceedance (AAE) of critical loads for acidification in 2000 (left) and 2020 under the Baseline Scenario (middle) and Maximum feasible reductions (right). Peaks of exceedances in 2000 on the Dutch-German border and in Poland (red shading) are reduced in 2020, as is the area at risk in general (size of shaded area in grid cells).

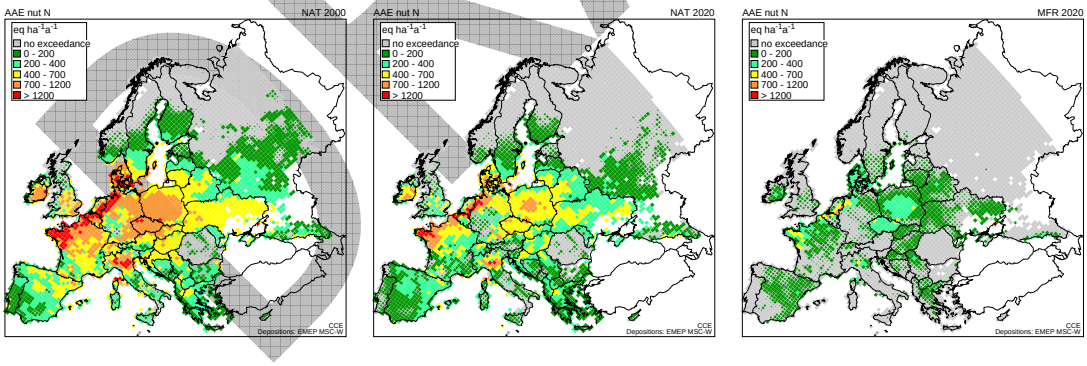

Figure 17: Average Accumulated Exceedance (AAE) of critical loads for eutrophication in 2000 (left), and in 2020 (NAT2020 data, middle) and MFR (MFR2020 data, right). The areas with peaks of exceedances in 2000 (red shading) are markedly decreased in 2020. However, area at risk of nutrient nitrogen (size of shades indicates relative area coverage) remain widely distributed over Europe in 2020, even under MFR.

As Figure 1 shows, ammonia is an important source of nitrogen to the environment. Figure 17 indicates ammonia concentrations expected under four projections. These models results show very little evolution between 2000 and 2020 under the baseline scenario. Even under MFR, very high concentrations (greater than 4 $\mu g.m^{-3}$) are still modelled in the Netherlands and in the Po valley. Under the baseline scenario, concentrations greater than the critical limit set for

bryophytes and lichen (1 µg.m^{-3}) are expected over most of Europe in 2020. Moreover concentrations greater than the critical limit set for higher plants (2-4 µg.m^{-3}) will also be found over large areas.

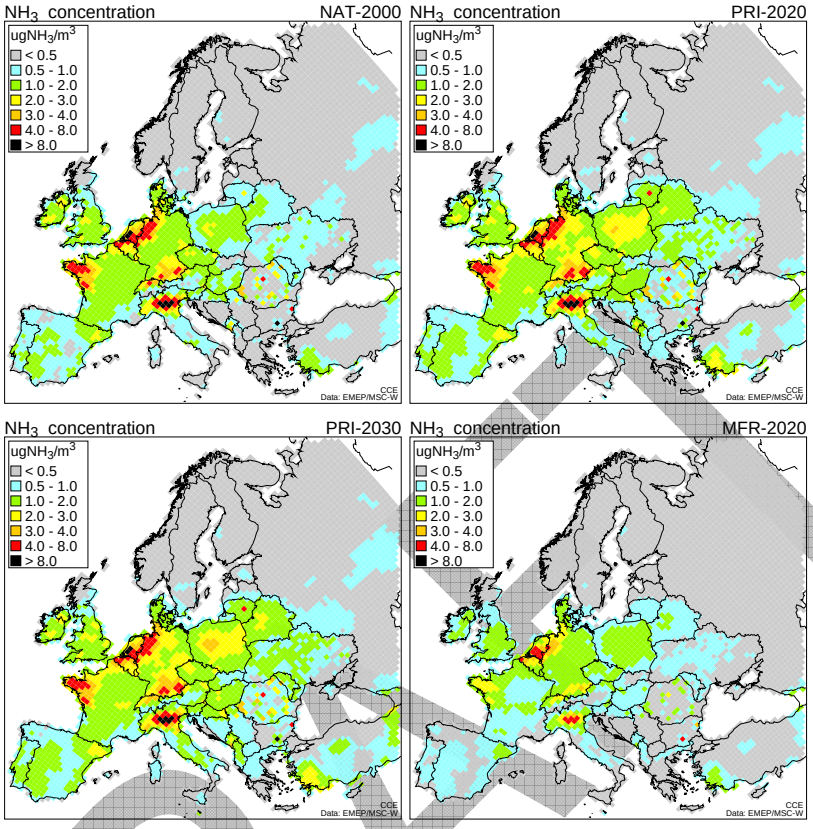

Figure 18: Ammonia concentrations under four projections and scenarios between 2000 and 2030. Critical limits for lichens and bryophytes is set at 1µg.m^{-3}. Critical limits for higher plants are set between 2 and 4 µg.m^{-3} (UBA, 2004, updated).

3.4.2 RISKS IN SIGNIFICANT CHANGE OF BIODIVERSITY.

The analysis of the change of biodiversity consists in a numerical estimation of the effects of scenario-specific nitrogen deposition in 2000 and 2020 (i) on the species richness of (semi-)natural grasslands (EUNIS class E), (ii) on the species richness of arctic and (sub-) alpine scrub habitats (EUNIS class F2) and (iii) on the Sorensen's similarity index of the understorey vegetation of coniferous boreal woodlands (EUNIS class G3 A-C). Thus "change of biodiversity" is used as a common name for any of these indicators.

This analysis is based on dose-response curves (Bobbink 2008, Bobbink and Hettelingh, 2011) that have been applied to these three EUNIS classes in Europe (Hettelingh et al. 2008a), using the European harmonized land cover map (Slootweg et al. 2009).

Here biodiversity change is considered significant if the indicator changed by more than 5% relative to its value in a control area (where the dose response curve has been established). The choice of 5% as a threshold percentage for identifying a "significant" change of biodiversity was arbitrary. It takes stock of widely applied statistical conventions regarding the analysis and representation of phenomena for which confidence levels need to be established.

The indicator thus derived is used only to evaluate the relative changes caused by differences between deposition scenarios. Uncertainties associated with its calculation prevent from using its absolute values. These uncertainties are discussed in Hettelingh et al (2011).

Results are shown on Figure 19 and in Table 6. The area at risk of a significant change of biodiversity evolves from covering many countries in 2000 to concerning predominantly the bordering area between Germany and the Netherlands in 2020 under MFR.

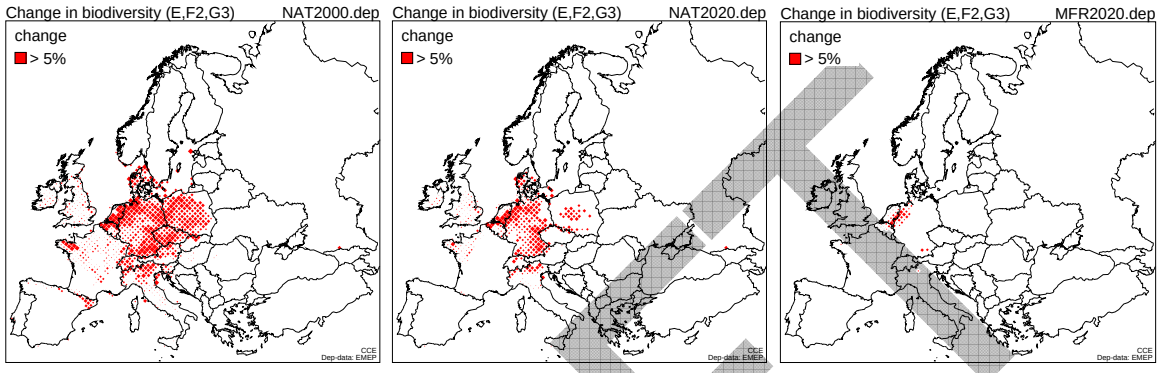

Figure 19: Change in biodiversity (all ecosystems) greater than 5%, caused by nitrogen deposition and evaluated with the NAT2000, NAT 2020 and MFR 2020 data sets.

Table 6: Areas tentatively computed to be at risk of a significant change of biodiversity in 2000 (col. II), in 2020 under the Baseline (col. III) and in 2020 under the Maximum Feasible Reductions (MFR) scenario (col. IV). The area at risk of a significant change of biodiversity in Europe in 2000, Baseline 2020 and MFR 2020 is about 5%, 2% and 0% respectively (last row). The improvement of the protection against the significant change of biodiversity under NAT2020 and MFR compared to 2000 is 4% (col. V) and 5% (col. VI) respectively.*

Species abundance or species richness	NAT2000	NAT2020	MFR2020	Environmental improvements compared to 2000	
	Area@risk of significant* Δ biodiv. (%)	Area@risk of significant* Δ biodiv. (%)	Area@risk of significant* Δ biodiv. (%)	CLE (%)	MFR (%)
	II	III	IV	V (II-III)	VI (II-IV)
EU27	15	6	1	9	15
All	9	4	0	6	9

*A change of 5 percent or more of species similarity in EUNIS class G3 or richness in EUNIS classes E and F2

3.4.3 THE RISK OF DELAYED EFFECTS RELATIVE TO 2050

Atmospheric processes are faster than soil processes, themselves occurring before any biological response may be observed. These different timings are taken into account by dynamic models and can be calculated. Thus, the delay between the time a critical load is exceeded and the time violation of the chemical

criterion in the soil is observed (for instance when the pollutant critical limit is reached or when N leaches) is called the damage delay time, or DDT. Similarly, when emissions are decreasing, depositions eventually drop below critical loads. As recovery is possible only when the chemical criterion is no longer violated, the recovery delay time (RDT) is the time lag between when depositions become lower than critical loads and when the chemical criterion is no longer violated. The various situations that can be observed are illustrated on Figure 20.

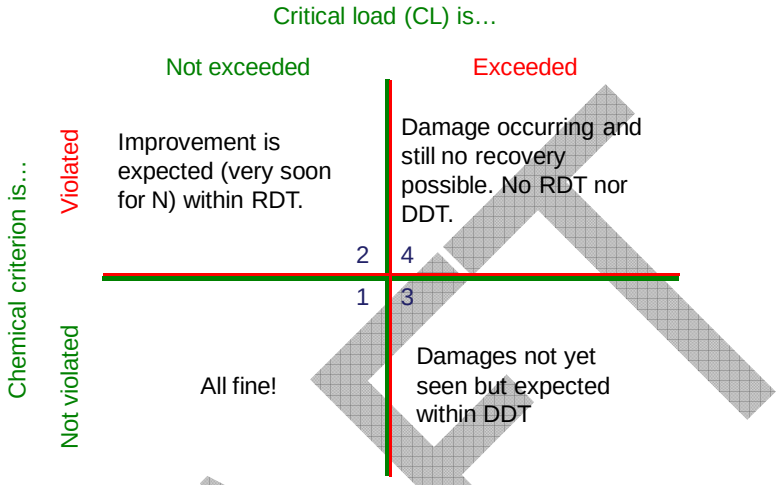

Figure 20: Four combinations of critical load (non-)exceedance and criterion (non-)violation. RDT: recovery delay time. DDT: damage delay time.

If 2050 is set as a future reference for evaluation of emission reduction, dynamic model can evaluate the areas where there are delays between depositions and violation of the chemical criterion. Results for the whole Europe are given in Table 7. MFR scenario shows significant improvement compared to the baseline.

Table 7: Natural areas in Europe with an RDT and DDT before or after 2050, under both NAT2020 and MFR2020, expressed as percentage of the area where critical loads for eutrophication are exceeded under baseline scenario in 2020.

Deposition and chemical criterion below critical thresholds (quadrant 1 of Figure 20).		Deposition has decreased below CLd. Recovery is expected (quadrant 2 of Figure 20).				Deposition has increased above critical loads, damages are expected (quadrant 3 of Figure 20).				Deposition is above critical loads. No calculated improvement (quadrant 4 of Figure 20).	
Safe in 2020		RDT≤ 2050		RDT> 2050		DDT>2050		DDT≤ 2050		Unrecoverable	
NAT 2020	MFR 2020	NAT 2020	MFR 2020	NAT 2020	MFR 2020	NAT 2020	MFR 2020	NAT 2020	MFR 2020	NAT 2020	MFR 2020
0	48	0	2	0	1	14	10	0	0	86	39

3.5 ICP VEGETATION

3.5.1 BACKGROUND

The indicators used in the Gothenburg Protocol to protect crops, trees and (semi-) natural vegetation from adverse impacts of ozone are based on the concentration metric, AOT40. Currently, only the SOMO 35 indicator for health and the AOT40 for trees (accumulated from April to September) are included in the GAINS model for reporting impacts of ozone. AOT40 has not been used as one of the effects-based indicators for optimisation. However, scientific research has developed significantly in the last decade and the accumulated ozone flux via leaf pores (stomatal flux) is now considered to provide a more biologically sound method for describing observed effects. It is calculated from the effects of climate (temperature, humidity, light), ozone, soil moisture availability and plant growth stage on the extent of opening of the stomatal pores through which ozone enters the plant. Led by the ICP Vegetation, several workshops held under the Working Group on Effects have developed ozone flux modelling methods and indicators for use in integrated assessment modelling.

In 2010, the accumulated ozone flux via leaf pores was renamed as the Phytotoxic Ozone Dose above a threshold of Y, POD_Y (previously described as $AF_{st}Y$) and nine flux-based critical levels for vegetation have been established (ECE/EB.AIR/WG.1/2010/13 ; Harmens et al., 2010; Mills et al., 2011b, and update of the *Manual on Methodologies and Criteria for Modelling and Mapping Critical Loads and Levels and Air Pollution Effects, Risks and Trends, UBA*). An analysis of over 500 records of ozone damage to vegetation in the field in 16 countries provides strong support for the use of the flux-based methodology (Hayes et al., 2007; Mills et al., 2011a). In addition, mapping of ozone flux in Europe indicated risks (supported by field evidence) in areas which would not be protected by the indicator for health effects of ozone (SOMO35) or by concentration-based critical levels (AOT40) for vegetation (Mills et al., 2008; Hayes et al., 2007, Mills et al., 2011a). Based on this evidence, the Executive Body of the Convention recommended the use of the flux-based methods for vegetation in the work on the revision of the Gothenburg Protocol (ECE/EB.AIR/96).

3.5.2 POLICY-RELEVANT EFFECT INDICATORS

Out of the nine flux-based critical levels, three were chosen specifically for use as policy-relevant indicators of ozone effects on vegetation (ECE/EB.AIR/WG.1 /2010/13; Harmens et al., 2010, LRTAP Convention, 2010). These were:

(a) **Agricultural crops**: the critical level for effects on the protein yield of wheat, a POD_6 of 2 mmol m^{-2}, used to protect the security of food supplies;

(b) **Forest trees**: the critical level for effects on whole tree biomass in beech and birch, a POD_1 of 4 mmol m^{-2}, used to protect against loss of carbon storage in living trees and loss of ecosystem services such as soil erosion, avalanche protection and flood prevention;

(c) **Grasslands, including pastures and areas of high conservation value**: the critical level for effects on the biomass of clover species, a POD_1 of 2 mmol m^{-2}, used to protect against loss of vitality and fodder quality in

productive grasslands and against loss of vitality of natural species in grasslands of high conservation value.

The ICP Vegetation recommends the use of these indicators for policy-related analysis. These critical levels have been derived using full flux models incorporating all climatic, soil and plant factor inputs. Soil moisture is an important influencing factor for stomatal flux and methods are currently under test for including it in the EMEP model. In the meantime, for use in large-scale and integrated assessment modelling, simplified flux models for generic species have also been derived that only include the effects of temperature, light, humidity and growth cycle on flux. These so-called *generic flux models* provide an indication of *areas at risk of damage* under "worst-case" conditions (i.e. assuming soil moisture is not limiting flux in any way) and are not recommended for economic impact assessment.

3.5.3 MAPPING DIFFERENT EFFECT INDICATORS USING THE VARIOUS PROJECTIONS

In this part of the report we compare the ozone flux-based risk maps for generic deciduous trees with the ozone concentration-based risk maps for forest trees (AOT40) and human health indicator (SOMO35).

Concentration-based maps using AOT40 or SOMO35 predict that southern European areas are most at risk from adverse ozone impacts (Figure 21 a and b). The ozone flux-based map indicates that in addition, large areas of central and northern Europe are also at risk from adverse ozone impacts (Figure 21 c), risks that are not predicted using AOT40 or SOMO35. This can be explained by the favourable climatic conditions (e.g. high humidity) that enhance ozone stomatal flux in northern (and central) Europe at moderate ozone concentrations. On the other hand, lower humidity and higher temperature in southern Europe tend to reduce stomatal ozone flux at relatively high ozone concentrations. This effect is even more pronounced when applying the MFR 2020 and the PRIMES 2030 scenarios (Figure 22). This important conclusion not only confirms previous results showing that policies aiming only at health effects would not protect vegetation in large areas of Europe (ECE/EB.AIR/96; Mills et al., 2008), but also indicates that the additional risk to vegetation in the northern third of Europe is of even more concern for future scenarios.

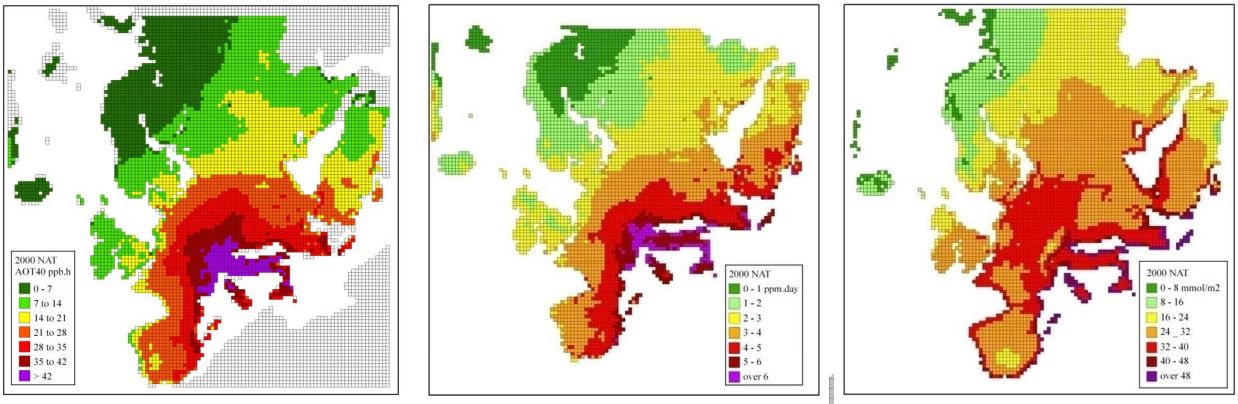

Figure 21: The risk of adverse ozone impacts in 2000 a) on biomass production in forest concentration-based AOT40 for forest trees (the AOT40-based critical level is 5 ppm.h), b) on human health as indicated by SOMO35, c) on generic deciduous tree as calculated by the flux model (POD1). The maps were produced using the NAT 2000 projection and colour classes have been scaled in the same way for each metric based on the highest values to allow direct comparison.

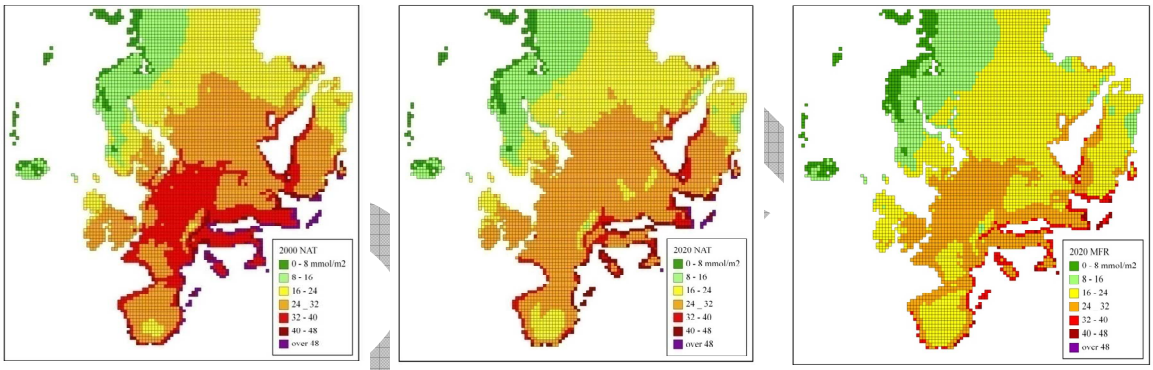

Figure 22: The risk of adverse ozone impacts on biomass production in forest using the generic deciduous tree flux model (POD_1) for a) NAT2000, b) NAT2020, c) MFR2020. Colour classes have been scaled in the same way for each metric based on the highest values to allow direct comparison.

Comparison of ozone risk maps for vegetation applying the different projections shows that despite the predicted reductions in both ozone concentrations and stomatal fluxes in the future, large areas in Europe will remain at risk from adverse impacts of ozone on vegetation, with areas at highest risk being predicted in parts of central and southern Europe. In Figure 23, the proportion of grid squares in each category illustrated on the maps is shown for the four scenarios. Although for the 2020 and 2030 scenarios there is a decrease in the proportion of grid squares in the highest categories, there remains > 25 % of grid squares in each of the two middle categories (16 – 24 and 24 – 32 mmol m^{-2}) indicating a continuing risk of damage. Hence, additional measures to reduce the emissions of ozone precursors will be required to protect large areas in Europe from adverse impacts of ozone on vegetation in 2020/30. According to the generic tree flux maps, the baseline scenario in 2020 (NAT2020 data) will reduce the severity of risk of ozone impacts on forests, but not so much the total area at risk of impacts. On the other hand, both the severity of risk of ozone impacts and the total area where they are

predicted to occur are reduced when the PRI2030 and especially the MFR2020 data are applied.

The ICP Vegetation also investigated the effects of ozone on wheat and tomato production using the same scenarios (Mills and Harmens, 2011). Figure 24 shows economic losses in million € per 50 x 50 km² grid square for wheat. These are for the full wheat flux model, assuming irrigation is used whenever soil moisture is limiting. The critical level of 1 mmol m^{-2} for effects on yield (above which loss in yield is above 5% according to ICP Vegetation (2010)) is exceeded in 85% of Europe in 2000 (NAT scenario, Figure 24 and Table 8) , and total economic losses of 3.2 billion € are predicted for EU27+CH+NO. Critical level exceedance is only reduced to 82% of grid squares in 2020 when applying the NAT projection, but the magnitude of the impact per grid square is decreased substantially reducing economic losses to 1.96 billion Euro in 2020 (NAT scenario).

Ozone impacts were also quantified for tomato as an example of a horticultural crop commonly grown in southern Europe (as well as in other countries such as the Netherlands and Belgium). Using the flux-based method, economic losses of 1.02 billion € representing 9.4% of production value were estimated for 2000 falling to 0.63 billion € in 2020 (NAT scenario, Table 8). The distribution of economic impacts on tomato are shown in Figure 25.

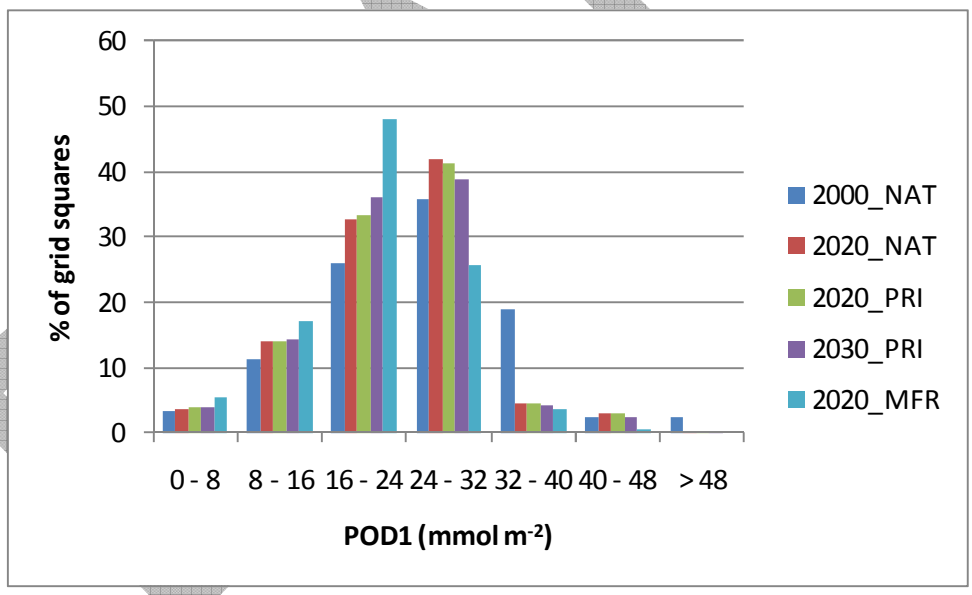

Figure 23: Proportion of grid squares within specified categories of POD1 calculated using the generic forest flux model as calculated with the different datasets.

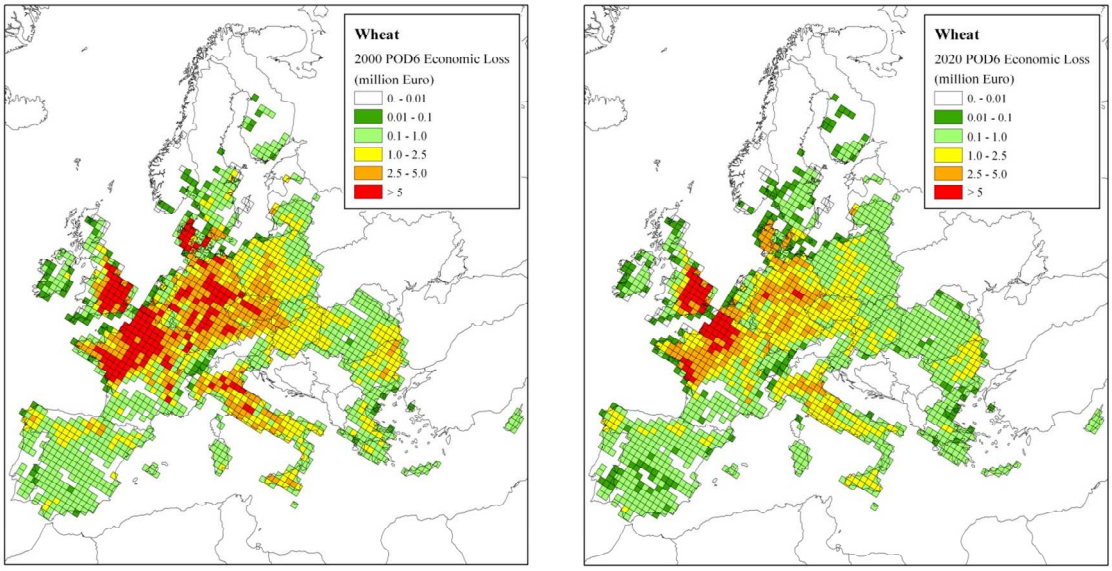

Figure 24: Predicted economic losses for ozone effects on wheat in million € per 50 x 50 km² grid square in (a) 2000 and (b) 2020 for the wheat growing areas of EU27+CH+NO as indicated by the NAT scenario and flux-based methodology (from Mills and Harmens, 2011).

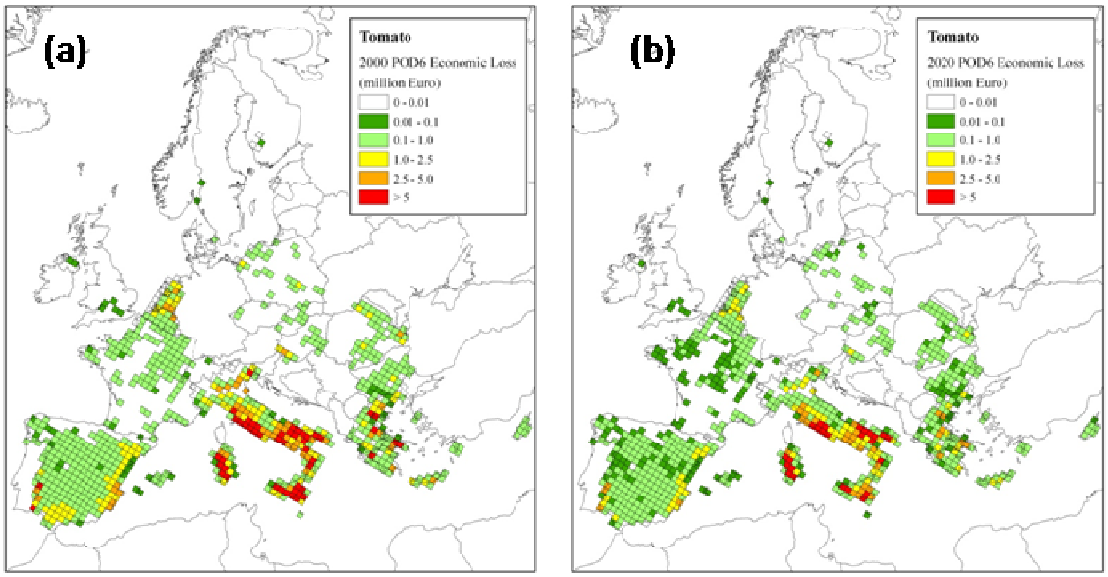

Figure 25: Predicted economic losses for effects on tomato in million Euro per 50 x 50 km grid square in (a) 2000 and (b) 2020 for the tomato growing areas of EU27+CH+NO (> 1 t yield per square) as indicated by the NAT scenario and flux-based methodology(from Mills and Harmens, 2011).

Table 8: Predicted impacts of ozone pollution on wheat and tomato yield and economic value, together with critical level exceedance in EU27+Switzerland+Norway in 2000 and 2020 under the current legislation scenario (NAT scenario). Analysis was conducted on a 50 x 50 km EMEP grid square using crop values in 2000 and an ozone stomatal flux-based risk assessment (From Mills and Harmens, 2011).

	Wheat		**Tomato**	
	2000	**2020**	**2000**	**2020**
Total production, million t	133.53		17.68	
Total economic value of wheat in 2000, billion Euro	15.87		6.85	
Mean % yield loss per grid square	13.7[1]	9.07[1]	9.4[2]	5.7[2]
Total production loss, million t	26.89	16.45	2.64	1.62
Total economic value loss, billion Euro	3.20	1.96	1.02	0.63
Percentage of EMEP grid squares exceeding critical level	84.8[1]	82.2[1]	77.8[2]	51.3[2]

[1]based on all grid squares with wheat production, [2] based on grid squares with > 1 tonne of production

3.5.4 TEMPORAL TRENDS

At the local scale there is evidence of higher ozone damage in years with higher ozone concentrations (e.g. 2003 and 2006) in regions in Europe where climatic conditions were conducive to high ozone fluxes (Hayes et al., 2007). However, there is no evidence of long-term trends related for example to the changing ozone profiles, i.e. lower peaks and higher background ozone concentrations (Royal Society, 2008).

3.5.5 OZONE IMPACTS IN A CHANGING CLIMATE BEYOND 2050

Apart from being a pollutant, ozone is also the third most important greenhouse gas, contributing to global warming. Hence, any measures to reduce the emissions of ozone will not only benefit air pollution but also climate change abatement policies. One main advantage of using the flux-based compared to the concentration-based approach for vegetation is that climate change factors (e.g. warming, relative humidity) affecting the opening of leaf pores and hence the uptake of ozone are included in calculating the ozone uptake by vegetation. Such factors are not included in the concentration-based indices.

One important challenge for the future is to investigate whether dose-response relationship established under current climatic conditions still hold in a future changing climate. There is an urgent need to include the impacts of ozone on vegetation in global climate models. Ozone pollution is likely to suppress the global carbon sink, leading to enhanced global warming (Sitch et al., 2007). Recent research has indicated that ozone concentrations within the ambient range might actually increase the opening of leaf pores , allowing increased ozone flux into the leaves and reducing drought tolerance in plants (Mills et al. 2009, Wilkinson & Davies, 2009, 2010). This may lead to water loss from vegetation being far greater than currently included in global climate models.

3.6 ICP MATERIALS

ICP Materials has established indicators for corrosion of materials based on carbon steel, zinc and limestone reaction to air pollution. These indicators are expressed as corrosion in µm for a one-year exposure based on a material sample exposure for in situ monitoring or calculated from dose-response relationships for modelling work. Multi-pollutant relationships (UBA2004 and updates, chapter 4) are used in the present analysis. They include the scenario dependent parameters SO_2, HNO_3 and PM10. The remaining parameters included in the dose-response relationships are temperature, relative humidity and hydrogen ion deposition due to precipitation (acid rain). In the present analysis, these last three parameters are considered scenario independent even if from a strict point of view they are scenario dependent. As they are not available from the scenarios provided by the TFIAM they have been derived from New et al (2002) for temperature, relative humidity and precipitation and by Kriging of station data for pH in precipitation.

ICP Materials has established three criteria that should be fulfilled for an indicator material. These are availability of (i) data on trends at ICP Materials test sites, (ii) reliable dose-response relationships, and (iii) acceptable and/or tolerable levels. These are all fulfilled for carbon steel, zinc and limestone but for soiling no single material fulfil all these criteria. Instead, a simplified synthesis of presently available data is used with PM10 as a material independent indicator for soiling based on the following general dose-response function:

$$\Delta R/R_0 = 1 - \exp(-k \cdot t \cdot PM10)$$

where $\Delta R/R_0$ is the loss in reflectance compared to an unsoiled surface, k is a material constant equal to (2.2 ± 0.2) x 10^{-3} (year µg m^{-3})$^{-1}$ based on data from limestone, painted steel and white plastic and t is the exposure time (Kucera et al, 2005).

Targets for corrosion and soiling in 2020 and 2050 are given in Table 9.

Table 9: Targets for protecting materials of infrastructure and cultural heritage for 2020 and 2050 (ECE/EB.AIR/WG.1/2009/16 "Indicators and targets for air pollution effects")

Indicator	2020	2050
Carbon steel corrosion	< 20 µm year^{-1}	< 16 µm year^{-1}
Zinc corrosion	< 1,1 µm year^{-1}	< 0,9 µm year^{-1}
Limestone corrosion	< 8,0 µm year^{-1}	< 6,5 µm year^{-1}
Soiling measured as loss in reflectance compared to an unsoiled surface	< 35% after 10 years	< 35% after 20 years

Table 10 shows overall compliances of targets for the EMEP region based on the dose-response relationships, data from the scenarios and the scenario-independent data. The last three entries in the table give a combined result for materials based on all the individual compliance results. These combined results for materials are also illustrated by Figure 26.

Table 10: Compliances of targets of indicators for materials calculated from dose-response relationships for the whole EMEP region in 2020.

Indicator and target	Nat 2000	Nat 2020	MFR 2020
Carbon steel corrosion, 2050 target met	94,2%	99,5%	99,9%
Carbon steel corrosion, 2020 target met (but not the 2050 target[(a)])	4,8%	0,5%	0,1%
Carbon steel corrosion, no target met	1,0%	0,0%	0,0%
Zinc corrosion, 2050 target met	70,6%	89,6%	97,2%
Zinc corrosion, 2020 target met[(a)]	28,1%	10,4%	2,8%
Zinc corrosion, no target met	1,3%	0,0%	0,0%
Limestone corrosion, 2050 target met	94,1%	97,8%	99,9%
Limestone corrosion, 2020 target met[(a)]	5,8%	2,2%	0,1%
Limestone corrosion, no target met	0,2%	0,0%	0,0%
Soiling, 2050 target met	70,6%	89,5%	97,2%
Soiling, 2020 target met[(a)]	27,8%	10,4%	2,8%
Soiling, no target met	1,6%	0,1%	0,0%
All 2050 targets met	66,7%	87,8%	95,4%
All 2020 targets met[(a)]	32,2%	11,9%	4,5%
No target met for at least one indicator	1,1%	0,3%	0,1%

(a): These lines indicate the areas where the 2020 targets are met but not the 2050 targets. Note that when 2050 targets are met, the 2020 target are also met. As a result, as deposition decreases, the % of areas where the 2050 target is met increases, to the expense of the % of areas where only the 2020 targets are met.

The 2050 targets are more difficult to meet than the 2020 targets, even though they are met at most locations (with the caveat of the urban area systematic difference as indicated in Table 5). Therefore when 2050 targets are met, 2020 targets are also met. The % indicated in Table 9 represent distribution of corrosion values. For instance, zinc has 2020 targets equal to 1.1 and 2050 targets equal to 0.9. The percentage values for NAT 2020 in table 4 (89.6%, 10.4% and 0%) just means that 89,6% of the calculated grids are below 0.9 and 10.4% between 0.9 and 1.1. So it is worth noting that only 20 to 30 % of the grid cells are between 0.9 and 1.1 (which is a relatively narrow range) and almost no values are above 1.1.

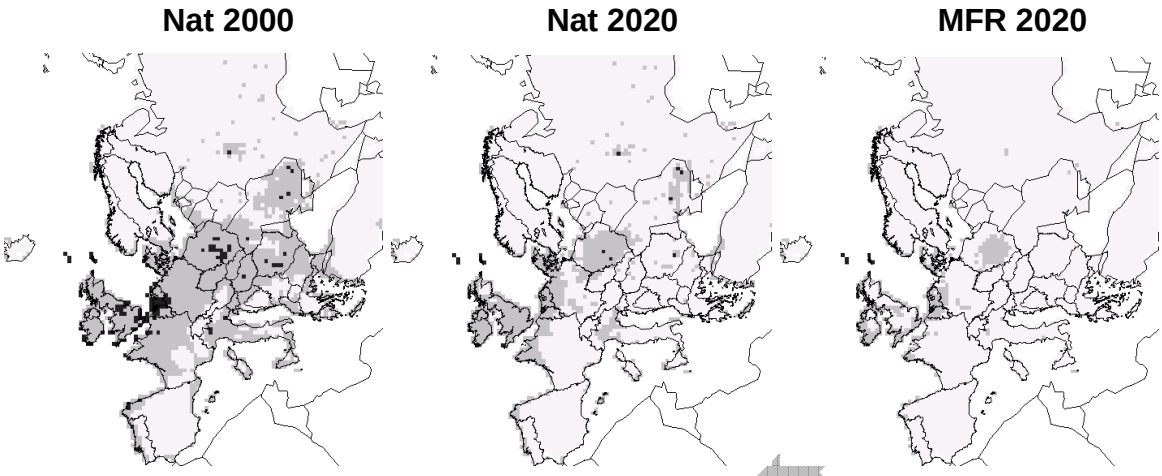

Figure 26: Compliances of targets of indicators for materials calculated from dose – response relationships for 2020 (light grey: All 2050 targets met; dark grey: All 2020 targets met (but 2050 targets not met); black: No target met for at least one indicator).

The results presented in Table 10 and Figure 26 show a picture with very few occurrences on non-compliance in 2020, especially if the MFR scenario was implemented. However, the comparatively large grid cell, 50 km x 50 km could have a significant impact on the results giving an underestimation of the pollution in urban areas and, as a consequence, greater corrosion/soiling where most of our cultural heritage is situated.

Therefore, a comparison of field observations and the calculated grid cell values has been performed for the year 2000 (Table 11). Percentiles in the distribution of SO_2 concentrations and of corrosion levels for carbon steel, zinc and limestone have been calculated and compared. For carbon steel, the 2050 target (16 µm, cf. Table 9) was met on 50% of the sites although calculations forecasted that it was reached in 75% of the grid cells. Results were similar for zinc and limestone. This suggests that sites were more severely impacted than the dose response function suggest using the data available here. The dose-response functions themselves are not the source for this error (Tidblad et al, 2010) but instead the underestimation of the SO_2 concentration possibly combined with differences in other environmental parameters between the site and the NAT 2000 data set.

Table 11: Comparison of field observations of SO_2 and corrosion of carbon steel, zinc and limestone at ICP Materials test sites for the year 2000 ("Field") and values for the same parameters calculated from the NAT 2000 dataset ("Nat") for the corresponding grid cells.

	SO_2 µg m^{-3}		**Carbon steel µm**		**Zinc µm**		**Limestone µm**	
	Nat	Field	Nat	Field	Nat	Field	Nat	Field
50-percentile	2	4	12	16	1,0	1,1	6,1	7,1
75-percentile	5	10	16	23	1,1	1,3	6,9	8,7
95-percentile	8	19	21	35	1,2	2,3	7,4	11,9

3.7 TASK FORCE ON HEALTH

The Task Force on Health (TF Health) discussed at its 13th Meeting the methods of health impact assessment (HIA) used currently to support the revision of the 1999 Gothenburg protocol and confirmed, in general, the validity of the GAINS model approaches. $PM_{2.5}$ and ozone were the two pollutants for which health impacts should be quantified.

Current version of the GAINS model indicates substantial impacts of PM on life expectancy. There are various observations demonstrating health benefits of air quality improvements. Particulate matter (PM) causes respiratory and cardiovascular mortality and morbidity and over 300,000 premature deaths are attributed to them every year in Europe. In the US, a recent study demonstrated that health improvement was associated with the decrease of PM levels over 20 years. In this study, a 7.3 months increase in life expectancy was attributed to a decrease of $PM_{2.5}$ by 10 $\mu g/m^3$ (Pope et al, 2009).

The Task Force on Health has compared the health risk associated with black carbon to that associated with $PM_{2.5}$. They concluded that although there is sufficient evidence of health risk associated with black carbon, it is insufficient to justify replacing $PM_{2.5}$ by black carbon as a health-relevant indicator of particulate air pollution.

Next to the all-cause mortality analysed by GAINS, cause-specific (cardiovascular, respiratory and lung cancer) estimates should be considered as a part of sensitivity analysis. The use of risk coefficients for $PM_{2.5}$ from the American Cancer Society (ACS) study is well justified as this study is based on the largest sample and has been a subject of thorough review and reanalysis. Support for its use was provided by the largest European cohort study to date (Brunekreef et al, 2009), which gives a risk estimate for all-cause mortality close to that from the ACS study.

The TF Health has assessed effects on human health of black carbon as a component of $PM_{2.5}$. It has found evidence of an association of black carbon (BC) variability with short-term changes of all cause and cardiovascular mortality, evidence of associations for all cause and cardiopulmonary mortality with long term average BC exposure, suggestive evidence that the effects of BC are (stronger) than those of PM_{10} or $PM_{2.5}$ but insufficient evidence on a potential difference in the mechanisms of effects of BC in comparison to those of other potentially toxic component of $PM_{2.5}$ and insufficient evidence to suggest any specific mechanism of effects of BC. As a result, the TF on Health has concluded that BC can not replace $PM_{2.5}$ as a health-relevant indicator of particulate air pollution.

Current calculations indicate that there are about 21 000 death per year in EU 25 accelerated by high concentrations (> 35 ppb or 70 $\mu g.m^{-3}$) of ozone. Only small decrease of the impacts can be expected as a result of the current policies.

The ozone HIA estimates should remain based on the SOMO35 indicator (annual sum of daily maximum mean eight-hour concentrations above 35 ppb), even though health impacts of ozone may occur at levels below 35 ppb. Recent studies suggest the impacts of long term exposure to ozone on respiratory symptoms and

on mortality due to respiratory diseases. If further studies confirm these long term health effects, expansion of GAINS model to take into consideration impacts of long term average ozone exposures on respiratory mortality should be considered in the future. The dose response relationships still need to be confirmed.

4. DISCUSSION AND CONCLUSIONS

4.1 SCIENTIFIC KNOWLEDGE: STATE OF THE ART

The Working Group on Effects has developed, compiled, collated large amount of scientific and multidisciplinary knowledge related to the impact of air pollution on ecosystems, human health and material. This work has been documented year after year in its ICPs and task force reports and summarised in the annual Working Group on Effects documentation.

The present assessment is the opportunity for an update and a focus of this knowledge. Thus, monitoring series presented and used here by ICP Forests, ICP Waters and ICP Integrated monitoring include the most recent measurements. Indicators and modelling approaches from all ICPs presented here have been developed (or improved) and validated under the Working Group on Effects and EMEP in the last 5 years or earlier. They are used for the first time to document and support policy decision for the revision of a protocol.

Salient points are:

- Flux based indicators of ozone damage on vegetation and crops (Phytotoxic ozone dose, POD_y) indicates that a large proportion of northern and central parts of Europe is at risk of ozone damage. This is underestimated by classical concentration based indicators (such AOT40). This conclusion is backed by evidence from field data collated by ICP Vegetation.
- Dynamic modelling allowed the assessment of recovery patterns and timing in aquatic and terrestrial ecosystems. It also made it possible to relate required deposition levels with chosen target year for recovery.
- Relative changes in biodiversity caused by nitrogen deposition have been quantified, from dose-response relationships applied to three types of ecosystems.
- An evaluation of material soiling and corrosion has been derived from dose-response relationships and set targets for the years 2020 and 2050.

Furthermore, the assessment of the Gothenburg scenarios has been an opportunity to compare monitoring data with modelled results. The renewed coherence of both types of results, shown here by ICP Waters and ICP Integrated monitoring, illustrates the robustness of the critical loads methodology.

Indicators recommended by the TF Health, the SOMO35 for ozone and relations between PM concentrations and year of life losses (YOLL) are currently taken into account in integrated assessment modelling. Present knowledge supports these two indicators and their use in the GAINS model so no new indicators were presented here to develop the information on air pollution impact on human health.

4.2 ON-GOING SCIENTIFIC PROGRESSES

It is a fact of life that science is always in progress. In the framework of the Working Group on Effects, the main paths that are undertaken are:

- Continuing monitoring: Long term monitoring, field measurements and epidemiology studies are required tools to understand processes that control long term processes involved in air pollution and its impacts on ecosystems, materials and human health.
- Nitrogen storage in soils and its eventual leaching to waters: Evaluation of nitrogen input and output fluxes show that nitrogen is accumulating in watersheds. Under continuous inputs, it is expected that soil storage capacity fills up and that, as a consequence, nitrogen leaches to surface waters. Modelling catchment potential for continued N accumulation will help to forecast (and potentially to prevent) N leaching and the resulting nutrient imbalance in aquatic ecosystems.
- Low levels of base cations observed in forests soils: Base cations are essential nutrients for plants. It is therefore essential to evaluate whether the modelled low values are confirmed by field measurements and whether they may contribute to low base cations levels in relevant freshwaters.
- New endpoints and indicators to reflect societal concerns: Air pollution impacts biodiversity and ecosystems services (such as water quality, carbon sequestration and recreational fisheries). Work in progress attempts to link such endpoints to critical loads and ozone concentrations.
- Assessment of impacts of air pollution under changing climate: it will necessary to:
    - Evaluate whether the dose-response relationships established for ozone under present climate conditions still holds in a future climate.
    - Model how climate change may slow or setback recovery from acidification on a large scale.
- Evaluation of the impacts of ozone:
    - on biodiversity and ecosystems services.
    - on vegetation in dynamic models.
    - on vegetation and crops in presence of excesses of nitrogen.
- Evaluation of rising background ozone impacts on:
    - On vegetation and crop yield.
    - Human health due to chronic exposure
- Evaluation of the impacts on materials of particulate matters in urban pollution hotspots.
- Evaluation of particulate matter on human health: in order to focus policies and to improve the effectiveness of their intervention, it is now necessary to consider particulate matter chemical and physical properties and their sources. In order to refine integrated assessment modelling, it may be considered to calculate separately impacts of mortality due to cardio-pulmonary diseases and lung cancer instead of one estimates for all causes of death.

4.3 POLICIES SUCCESSES MONITORED BY THE WORKING GROUP ON EFFECTS

Measurements in the field remain the most effective and robust approach to monitor the effects of air policy on the environment. Thus, the first and most direct consequence of pollutant emission reductions, the decrease of sulphur deposition, is now clearly recorded across several regions in Europe thanks to long–running observations at ICP Forests, ICP Waters and ICP Integrated monitoring sites.

Following the decrease of sulphur emissions to the atmosphere, the trends in several chemical indicators (such as pH, ANC) have been reversed: at many ICP Waters sites, pH and ANC are now increasing whereas they were decreasing in the 1980s and early 1990s. Biological recovery is still fragile but nevertheless on going in several parts of Europe (cf. for instance Figure 8 and Table 2).

Response of terrestrial ecosystems seems somewhat slower: Soil water pH on ICP Forests plots still exceeds critical limits for forests on half of the monitored plots (Fischer et al., 2010). Furthermore, a comparison between two surveys on over 2000 level I plots showed that significant improvements in soil solid phase pH have been observed only on strongly acidified soils with pH below 4.0 between the end of the 1990s and the years 2004 to 2008 (De Vos and Cools, 2011).

Past policies have been less stringent on nitrogen emission reductions than on sulphur. This is also observed in the field: at 80% of ICP Forests level II sites, nitrogen depositions showed no significant changes between 1998 and 2007 (Fischer et al., 2010).

Models results complete the information obtained in the field. Modelling carried out by all ICPs clearly shows the important decrease of areas at risk of acidification, and, to a lesser extend although still significant, the decrease of areas at risk of eutrophication since 2000.

Ozone affects both human health and vegetation growth. It is formed in the atmosphere in the presence of sunlight, NOx, and volatile organic compounds. Long term measurements indicate small decrease in peak ozone concentration but rising background ozone concentrations. Recent modelling and monitoring work by ICP Vegetation has shown that ozone impacts were widespread in Europe and not mainly confined to southern European countries. Impacts on human health are taken into account in integrated modelling, via the SOMO 35 indicator in accordance with the work carried out by the TF Health.

As for PM, the TF Health has reported that improvement of air quality accounted for 15 % of the overall increase in life expectancy in the US between 1980 and 2000 (Pope AC et al., 2009). These north American results are corroborated by a recent European study (Nawrot et al., 2011). Also, evidence is at the moment insufficient to evaluate the specific impact of black carbon on human health but the TF on Health recommends that PM2.5 concentrations remain the indicator for human health. It should not be replaced, at present, by black carbon concentrations.

4.4 SCENARIOS ANALYSIS INFORMS ON THE IMPACT OF FUTURE REGULATIONS

Models run by the Working Group on Effects provide an insight into the potential impacts, or recovery, that may be expected from the implementation of policies. The first result is that improvements of the condition of the environment (in terms

of acidification, eutrophication and ozone impact) are expected by 2020 even if regulations lead only to emission reductions considered in the least ambitious baseline scenario. In that scenario, little improvement of human health is expected as far as ozone effects are concerned.

The second result of importance is that none of the scenarios considered would allow full recovery of the ecosystems. Even with the MFR scenario, the areas at risk of acidification in Europe would be greater than 2% and the most acidified sites of ICP Waters and ICP Integrated monitoring would not recover. About 20% of the European area would still be at risk of eutrophication. Critical levels of ozone for vegetation will still be exceeded in large areas of Europe, including in >80% of the wheat growing areas Also in about 5% of the European area the 2050 targets for materials would not be met.

The present analysis is the fruit of a robust collaboration between groups under EMEP and the Working Groups on Effects, responding to WGSR needs for information. It is a preliminary study as the deposition values used for the modelling were issued from scenarios prepared in October 2010.

Since October 2010, following the WGSR requests, CIAM and the TF IAM have been recalculating baselines, MFR and intermediate scenarios. Once new scenarios are validated by the WGSR, the WGE propose to run again their models and to provide final estimations. It is expected that absolute values will change with the new calculations but that main trends will remain as described in this document.

5. BIBLIOGRAPHY

Achermann, B., Bobbink, R., 2003. Empirical critical loads for nitrogen. Proceedings from the expert workshop Bern Switzerland Nov 11-13 2002. Environmental Documentation no 164 Air. Swiss Agency for the Environment, Forest and Landscape. http://www.bafu.admin.ch/publikationen/publikation/00252/index.html?lang=en

Amann M, Bertok I, Cofala J, Heyes C, Klimont Z, Rafaj P, Schöpp W, Wagner F, 2010. Scope for further environmental improvements in 2020 beyond the baseline projections, Background paper for the 47th Session of the Working Group on Strategies and Review of the Convention on Long-range Transboundary Air Pollution, Geneva, August 30 – September 3 2010, Centre for Integrated Assessment Modelling (CIAM), International Institute for Applied Systems Analysis (IIASA), CIAM Report 1/2010, http://gains.iiasa.ac.at/index.php/publications/policy-reports/gothenburg-protocol-revision.

Amann, M., Bertok, I., Borken-Kleefeld, J., Cofala, J., Heyes, C., Höglund-Isaksson, L., Klimont, Z., Rafaj, P., Schöpp, W., et Wagner, F. (2011). "Cost-effective Emission Reductions to Improve Air Quality in Europe in 2020. Scenarios for the Negotiations on the Revision of the Gothenburg Protocol under the Convention on Long-range Transboundary Air Pollution." IIASA, International institute for applied systems analysis, Laxenburg, Austria.

Bonten L, Posch M, Reinds GJ (2009). Dynamic modelling of effects of deposition on carbon sequestration and nitrogen availability: VSD plus C and N dynamics (VSD+). In: Hettelingh JP, Posch M, Slootweg J (eds.) (2009) Progress in the modelling of critical thresholds, impacts to plant species diversity and ecosystem services in Europe: CCE Status Report 2009, Coordination Centre for Effects, www.pbl.nl/cce

Brunekreef, B., Beelen, R., Hoek, G., Schouten, L., Bausch-Goldbohm, S., Fischer, P., Armstrong, B., Hughes, E., Jerrett, M., et van den Brandt, P. (2009). "Effects of Long-Term Exposure to Traffic-Related Air Pollution on Respiratory and Cardiovascular Mortality in the Netherlands: The NLCS-AIR Study". Health Effects Institute, Boston, USA. HEI Research Report 39.

Cosby, B. J., R. C. Ferrier, A. Jenkins, and R. F. Wright. 2001. Modelling the effects of acid deposition: refinements, adjustments and inclusion of nitrogen dynamics in the MAGIC model. Hydrology and Earth System Sciences 5:499-518.

Cosby, B. J., G. M. Hornberger, J. N. Galloway, and R. F. Wright. 1985. Modelling the effects of acid deposition: assessment of a lumped parameter model of soil water and streamwater chemistry. Water Resources Research 21:51-63.

De Vos, N. and Cools, B. 2011: European Forest Soil Condition Report. in press.

Fischer R, Lorenz M, Granke O, Mues V, Iost S, Van Dobben H, Reinds GJ, De Vries W (2010). Forest Condition in Europe, 2010 Technical Report of ICP Forests. Work Report of the Institute for World Forestry 2010/1. ICP Forests, Hamburg, 2010, 175pp.

Gundersen P, Sevel L, Christiansen JR, Vesterdal L, Hansen K, Bastrup-Birk A (2009). Do indicators of nitrogen retention and leaching differ between coniferous and broadleaved forests in Denmark? Forest Ecology and Management 258 (2009) 1137–1146

Henriksen, A., Posch, M., 2001. Steady-state models for calculating critical loads of acidity for surface waters. Water, Air, and Soil Pollution: Focus 1:375-398.

Hesthagen, T., Fjellheim, A., Schartau, A. K., Wright, R. F., Saksgård, R., et Rosseland, B. O. (2011). Chemical and biological recovery of Lake Saudlandsvatn, a formerly highly acidified lake in southernmost Norway, in response to decreased acid deposition. Science of The Total Environment Vol. 409, 2908-2916.

Hettelingh, J. P., Posch, M., Slootweg, J., et Le Gall, A. C. (2011). Analysis of environmental impacts caused by the Baseline and Maximum Feasible Reduction Scenarios. In "CCE Status report", pp. 15. RIVM, Bilthoven, Pays Bas.

Hindar, A., and R. F. Wright. 2005. Long-term records and modelling of acidification, recovery, and liming at Lake Hovvatn, Norway. Canadian Journal of Fisheries and Aquatic Sciences 62:2620-2631.

Holmberg, M., Posch, M., Kleemola, S., Vuorenmaa, J., Forsius, M., 2009. Calculation of critical loads for acidification and eutrophication for terrestrial and aquatic ecosystems. In: Kleemola, S. and Forsius, M. (Eds.) ICP IM 18th Annual Report. The Finnish Environment 23/2009. p. 23-35.

ICP Vegetation (2010). "Flux-based assessment of ozone effects for air pollution policy", pp6, Rep. No. ECE/EB.AIR/WG.1/2010/13. International Cooperative Programme on Effects of Air Pollution on Natural Vegetation and Crops, Convention on long range transboundary air pollution.

IEA (2009). "World Energy Outlook 2009." OECD/International Energy Agency, Paris, France.

Iost, S., Rautio, P., Lindroos A.-J. (2011): Spatio-temporal trends in soil solution chemistry in relation to critical limits in European forest soils. Submitted to Water, Air, and Soil Pollution

Kucera V, Tidblad J, Samie F, Schreiner M, Melcher M, Kreislova K, Knotkova D, Lefèvre R-A, Ionescu A, Snethlage R, Varotsos C, De Santis F, Mezinskis G, Sidraba I, Henriksen J, Kobus J, Ferm M, Faller M, Reiss D, Yates T, Watt J, Hamilton R & O´Hanlon S, 2005. MULTI-ASSESS publishable final report. URL: http://www.corr-institute.se/MULTI-ASSESS/.

Mills, G., Harmens, H. (eds). (2011). Ozone pollution: A hidden threat to food security. Programme Coordination Centre for the ICP Vegetation, Centre for Ecology and Hydrology, Bangor, UK. ISBN 978-1-906698-27-0.

Mills, G., Hayes, F., Simpson, D., Emberson, L., Norris, D., Harmens, H., Büker, P. (2011a). Evidence of widespread effects of ozone on crops and (semi-)natural vegetation in Europe (1990 - 2006) in relation to AOT40 - and flux-based risk maps. Global Change Biology 17: 592-613.

Mills, G., Pleijel, H., Braun, S., Büker, P., Bermejo, V., Calvo, E., Danielsson, H., Emberson, L., González Fernández, I., Grünhage, L., Harmens, H., Hayes, F., Karlsson, P.-E., Simpson, D. (2011b). New stomatal flux-based critical levels for ozone effects on vegetation. Atmospheric Environment 45: 5064-5068.

Nawrot, T. S., Perez, L., Künzli, N., Munters, E., et Nemery, B. (2011). Public health importance of triggers of myocardial infarction: a comparative risk assessment. The Lancet Vol. 377, 732:740.

New M, Lister D, Hulme M & Makin I, 2002. A high-resolution data set of surface climate over global land areas, Climate Research, Vol. 21, pp. 1–25.

Pope, C. A., Ezzati, M., et Dockery, D. W. (2009). Fine-Particulate Air Pollution and Life Expectancy in the United States. Vol. 360, pp. 376-386.

Posch M, Hettelingh J-P, De Smet PAM, 2001. Characterization of critical load exceedances in Europe. Water, Air and Soil Pollution 130: 1139-1144

Skjelkvåle, B. L., et de Wit, H., eds. (2008). "ICP Waters: 20 years of monitoring effects of long-range transboundary air pollution on surface waters in Europe and North America", pp. 1-55. International Cooperative Programme on assessment and monitoring of acidification of rivers and lakes, Convention on long-range transboundary air pollution, Oslo, Norway.

Schöpp W, Posch M, Mylona S, Johansson M, 2003. Long-term development of acid deposition (1880-2030) in sensitive freshwater regions in Europe. Hydrology and Earth System Sciences 7(4): 436-446

Tidblad J, De la Fuente D, Faller M and Kreislova K. ICP Materials Report No 64 Validity of dose-response functions for different climatic conditions, Swerea KIMAB, 2010

UBA 2004, updated. Manual on methodologies and criteria for modelling and mapping critical loads and levels and air pollution effects, risks and trends. UNECE Convention on Long-range Transboundary Air Pollution, Federal Environmental Agency (Umweltbundesamt), Berlin. http://www.icpmapping.org

Vuorenmaa, J., Kleemola, S., Forsius, M., 2009. Trend assessment of bulk deposition, throughfall and runoff water/soil water chemistry at ICP IM sites In: Kleemola, S. and Forsius, M. (Eds.) 18th Annual Report 2009. ICP Integrated Monitoring. The Finnish Environment 23/2009, pp. 36-63. Finnish Environment Institute, Helsinki.

Wright, R. F., C. Alewell, J. Cullen, C. D. Evans, A. Marchetto, F. Moldan, A. Prechtel, and M. Rogora. 2001. Trends in nitrogen deposition and leaching in acid-sensitive streams in Europe. Hydrology and Earth System Sciences 5:299-310.

Wright, R. F., T. Larssen, L. Camarero, B. J. Cosby, R. C. Ferrier, R. C. Helliwell, M. Forsius, A. Jenkins, J. Kopácek, V. Majer, F. Moldan, M. Posch, M. Rogora, and W. Schöpp. 2005. Recovery of acidified European surface waters. Envzironmental Science & Technology 39:64A-72A.